NATIONAL ADVISORY COMMITTEE FOR AERONAUTICS

WARTIME REPORT

ORIGINALLY ISSUED
August 1945 as
Advance Restricted Report L5F23

LIFTING-SURFACE-THEORY VALUES OF THE DAMPING IN ROLL AND OF THE PARAMETER USED IN ESTIMATING AILERON STICK FORCES

By Robert S. Swanson and E. LaVerne Priddy

Langley Memorial Aeronautical Laboratory
Langley Field, Va.

NACA

WASHINGTON

NACA ARR No. L5F23 [redacted]

NATIONAL ADVISORY COMMITTEE FOR AERONAUTICS

ADVANCE RESTRICTED REPORT

LIFTING-SURFACE-THEORY VALUES OF THE DAMPING IN ROLL AND OF THE PARAMETER USED IN ESTIMATING AILERON STICK FORCES

By Robert S. Swanson and E. LaVerne Priddy

SUMMARY

An investigation was made by lifting-surface theory of a thin elliptic wing of aspect ratio 6 in a steady roll by means of the electromagnetic-analogy method. From the results, aspect-ratio corrections for the damping in roll and aileron hinge moments for a wing in steady roll were obtained that are considerably more accurate than those given by lifting-line theory. First-order effects of compressibility were included in the computations.

The results obtained by lifting-surface theory indicate that the damping in roll for a wing of aspect ratio 6 is 13 percent less than that given by lifting-line theory and 5 percent less than that given by lifting-line theory with the edge-velocity correction derived by Robert T. Jones applied. The results are extended to wings of other aspect ratios.

In order to estimate aileron stick forces from static wind-tunnel data, it is necessary to know the relation between the rate of change of hinge moments with rate of roll and rate of change of hinge moments with angle of attack. The values of this ratio were found to be very nearly equal, within the usual accuracy of wind-tunnel measurements, to the values estimated by using the Jones edge-velocity correction, which for a wing of aspect ratio 6 gives values 4.4 percent less than those obtained by lifting-line theory. An additional lifting-surface-theory correction was

[redacted]

calculated but need not be applied except for fairly large high-speed airplanes.

Simple practical methods of applying the results of the investigation to wings of other plan forms are given. No knowledge of lifting-surface theory is required to apply the results. In order to facilitate an understanding of the procedure, an illustrative example is given.

INTRODUCTION

One of the many aerodynamic problems for which a theoretical solution by means of lifting-line theory might be expected to be inadequate is the case of a wing in steady roll. Robert T. Jones has obtained in an unpublished analysis similar to that of reference 1 a correction to the lifting-line-theory values of the damping in roll that amounts to an 8-percent reduction in the values for a wing of aspect ratio 6. Still more accurate values may be obtained by use of lifting-surface theory.

A method of estimating aileron stick forces in a steady roll from static wind-tunnel data on three-dimensional models is presented in reference 2. This method is based upon the use of charts giving the relation between the rate of change of hinge moment with rate of roll C_{h_p} and the rate of change of hinge moment with angle of attack C_{h_α} in the form of the parameter $(\alpha_p)_{C_h} = \left|\frac{C_{h_p}}{C_{h_\alpha}}\right|$, which is determined by means of lifting-line theory. It was pointed out in reference 2 that the charts might contain fairly large errors which result from neglecting the chordwise variation in vorticity and from satisfying the airfoil boundary conditions at only one point on the chord as is done in lifting-line theory. A more exact determination of the parameter $(\alpha_p)_{C_h}$ is desired. In reference 3 an additional aspect-ratio correction to C_{h_α} as determined from lifting-surface theory is presented. In order to evaluate the possible errors in the values of $(\alpha_p)_{C_h}$

as determined by lifting-line theory, it is necessary to determine similar additional aspect-ratio corrections to C_{h_p}.

A description of the methods and equipment required to solve lifting-surface-theory problems by means of an electromagnetic analogy is presented in reference 4. An electromagnetic-analogy model simulating a thin elliptic wing of aspect ratio 6 in a steady roll was constructed (fig. 1) and the magnetic-field strength simulating the induced downwash velocities was measured by the methods of reference 4. Data were thus obtained from which additional aspect-ratio corrections to C_{h_p} for a wing of aspect ratio 6 were determined.

Because of the small magnitude of the correction to $(\alpha_p)_{C_h}$ introduced by the lifting-surface calculations, it was not considered worth while to conduct further experiments on wings of other plan forms. An attempt was therefore made to effect a reasonable generalization of the results from the available data.

Inasmuch as the theory used in obtaining these results is rather complex and an understanding of the theory is not necessary in order to make use of the results, the material presented herein is conveniently given in two parts. Part I gives the results in a form suitable for use without reference to the theory and part II gives the development of the theory.

SYMBOLS

α	angle of attack (radians, unless otherwise stated)
c_l	section lift coefficient $\left(\frac{\text{Lift}}{qc}\right)$
C_L	wing lift coefficient $\left(\frac{\text{Lift}}{qS}\right)$
C_h	hinge-moment coefficient $\left(\frac{\text{Hinge moment}}{q\bar{c}_a^2 b_a}\right)$
C_l	rolling-moment coefficient $\left(\frac{\text{Rolling moment}}{qSb}\right)$

a_o slope of the section lift curve for incompressible flow, per radian unless otherwise stated

$pb/2V$ wing-tip helix angle, radians

Γ circulation strength

C_{l_p} damping coefficient; that is, rate of change of rolling-moment coefficient with rate of roll $\left(\frac{\partial C_l}{\partial (pb/2V)}\right)$

C_{h_p} rate of change of hinge moment with rate of roll $\left(\frac{\partial C_h}{\partial (pb/2V)}\right)$

C_{h_α} rate of change of hinge moment with angle of attack $\left(\frac{\partial C_h}{\partial \alpha}\right)$

C_{L_α} rate of change of wing lift coefficient with angle of attack $\left(\frac{\partial C_L}{\partial \alpha}\right)$

$(\alpha_p)_{C_h}$ absolute value of the ratio $\left(\frac{C_{h_p}}{C_{h_\alpha}}\right)$

c wing chord

c_s wing chord at plane of symmetry

c_b balance chord of aileron

c_a chord of aileron

$\overline{c}_a$ aileron root-mean-square chord

x chordwise distance from wing leading edge

y spanwise distance from plane of symmetry

b_a aileron span

$b/2$ wing semispan

S	area of wing
W	weight of airplane
F_s	stick force, pounds
θ_s	stick deflection, degrees
δ_a	aileron deflection, degrees, positive downward
A	aspect ratio
A_c	equivalent aspect ratio in compressible flow $\left(A\sqrt{1 - M^2}\right)$
λ	taper ratio, ratio of fictitious tip chord to root chord
M	free-stream Mach number
w	vertical component of induced velocity
V	free-stream velocity
q	free-stream dynamic pressure $\left(\frac{1}{2}\rho V^2\right)$
E	edge-velocity correction factor for lift
E'	edge-velocity correction factor for rolling moment
F	hinge-moment factor for theoretical load caused by streamline-curvature correction (reference 5)
η	experimentally determined reduction factor for F to include effects of viscosity
ϕ	trailing-edge angle, degrees
θ	parameter defining spanwise location $\left(\cos^{-1}\frac{y}{b/2}\right)$
K_1, K_2	constants

Subscripts:

LL	lifting-line theory

LS	lifting-surface theory
EV	edge-velocity correction
SC	streamline curvature
max	maximum
o	outboard
i	inboard
e	effective
c	compressibility equivalent

I - APPLICATION OF METHOD TO STICK-FORCE ESTIMATIONS

GENERAL METHOD

The values of the damping in roll C_{l_p} presented in reference 2 were obtained by applying the Jones edge-velocity correction to the lifting-line-theory values. For a wing of aspect 6, the Jones edge-velocity correction reduces the values of C_{l_p} by about 8 percent. From the data obtained on the electromagnetic-analogy model of the elliptic wing of aspect ratio 6, a more accurate correction to C_{l_p} for this aspect ratio could be calculated. The damping in roll was found to be 13 percent less than that given by lifting-line theory. The results were extended to obtain values of C_{l_p} for wings of various aspect ratios and taper ratios. These values are presented in figure 2. The parameter $\sqrt{1 - M^2}$ is included in the ordinates and abscissas to account for first-order compressibility effects. The value of a_o to be used in figure 2 is the value at $M = 0$.

The method of estimating aileron stick forces requires the use of the parameter $(\alpha_p)_{C_h} = \left|\frac{C_{h_p}}{C_{h_\alpha}}\right|$.

Because C_{h_α} can be found from the static wind-tunnel data, it is possible to determine C_{h_p} and thus the effect of rolling upon the aileron stick forces if $(\alpha_p)_{C_h}$ is known. In order to avoid measuring C_{h_α} at all points to be computed, the effect of rolling is usually accounted for by estimating an effective angle of attack of the rolling wing such that the static hinge moment at this angle is equivalent to the hinge moments during a roll at the initial angle of attack. The effective angle of attack is equal to the initial angle of attack corrected by an incremental angle $(\Delta\alpha)_{C_h}$ that accounts for rolling, where

$$(\Delta\alpha)_{C_h} = (\alpha_p)_{C_h} \frac{pb}{2V} \qquad (1)$$

The value of $(\Delta\alpha)_{C_h}$ is added to the initial α for the downgoing wing and subtracted from the initial α for the upgoing wing. The values of C_h corresponding to these corrected values of α are then determined and are converted to stick force from the known dynamic pressure, the aileron dimensions, and the mechanical advantage.

The value of $pb/2V$ to be used in equation (1) for determining $(\Delta\alpha)_{C_h}$ is (as explained in reference 2) the estimated value for a rigid unyawed wing; that is,

$$\frac{pb}{2V} = \frac{C_l}{C_{l_p}}$$

The value of C_l to be used in calculating $pb/2V$ should also be corrected for the effect of rolling. The calculation of $pb/2V$ is therefore determined by successive approximations. For the first approximation, the static values of C_l are used with the value of C_{l_p} from figure 2. From the first-approximation values of $pb/2V$, an incremental angle of attack $(\Delta\alpha)_{C_l}$ is estimated. For all practical purposes,

$$(\alpha_p)_{C_l} = (\alpha_p)_{C_h}$$

and from equation (1),

$$(\Delta\alpha)_{C_l} = (\alpha_p)_{C_h} \frac{pb}{2V}$$

Second-approximation values of C_l can be determined at the effective angles of attack $\alpha + \Delta\alpha$ and $\alpha - \Delta\alpha$. The second-approximation value of $pb/2V$ obtained from this value of C_l is usually sufficiently accurate to make further approximations unnecessary.

In order to estimate the actual rate of roll, values of $pb/2V$ for the rigid unyawed wing must be corrected for the effects of wing flexibility and airplane yawing motion. An empirical reduction factor of 0.8 has been suggested for use when data on wing stiffness and stability derivatives are not available to make more accurate corrections. Every attempt should be made to obtain such data because this empirical reduction factor is not very accurate - actual values varying from 0.6 to 0.9. The improvement in the theoretical values of C_{l_p} obtained by use of lifting-surface theory herein is lost if such an empirical factor is used. In fact, if more accurate corrections for wing twist and yawing motion are not made, the empirical reduction factor should be reduced to 0.75 when the more correct values of C_{l_p} given in figure 2 are used.

The values of $(\alpha_p)_{C_h}$ presented in reference 2 were obtained by graphically integrating some published span-load curves determined from lifting-line theory. Determination of this parameter by means of the lifting-surface theory presented herein, however, gives somewhat more accurate values and indicates a variation of the parameter with aspect ratio, taper ratio, aileron span, Mach number, C_{h_α}, and the parameter $\frac{F\eta}{(c_a/c)^2}$

In practice, a value of $(\alpha_p)_{C_h}$ equal to the lifting-line-theory value of $(\alpha_p)_{C_{h_{LL}}}$ (see appendix) times the Jones edge-velocity correction parameter $\frac{A_c + 4}{A_c + 2} \frac{A_c E_c + 2}{A_c E'_c + 4}$ is probably sufficiently accurate. The incremental angle of attack $(\Delta\alpha)_{C_h}$ is then

$$(\Delta\alpha)_{C_h} = \frac{pb}{2V}\left(\alpha_p\right)_{C_{h_{EV}}}$$

$$= \left(\alpha_p\right)_{C_{h_{LL}}} \frac{A_c + 4}{A_c + 2} \frac{A_c E_c + 2}{A_c E'_c + 4} \frac{pb}{2V} \qquad (2)$$

If further refinement in estimating the stick force is desired, a small additional lifting-surface-theory correction $\Delta C_h = \Delta\left(C_{h_p}\right)_{LS} \frac{pb}{2V}$ may be added to the hinge moments determined. For wings of aspect ratios of from about 4 to 8, values of this additional lifting-surface-theory correction are within the usual accuracy of the measurements of hinge moments in wind tunnels; that is,

$$\Delta C_h = \Delta\left(C_{h_p}\right)_{LS} \frac{pb}{2V} \approx 0.002$$

for a pb/2V of 0.1 and therefore need not be applied except for very accurate work at high speeds on large airplanes. Values of $\left(\alpha_p\right)_{C_{h_{LL}}} \frac{A_c + 4}{A_c + 2}$ are given in figure 3. The effective aspect ratio $A_c = A\sqrt{1 - M^2}$ is used to correct for first-order compressibility effects and values of $\frac{A_c E_c + 2}{A_c E'_c + 4}$ are given as a function of A_c in figure 4. Values of the correction

$$\Delta\left(C_{h_p}\right)_{LS} \frac{(c_a/c)^2}{F\eta}\sqrt{1 - M^2}$$

are given in figure 5 as a function of A_c, and values of $\frac{F}{(c_a/c)^2}$ are given in figure 6. The value of η is approximately $1 - 0.0005\phi^2$. The values of c_b/c_a given in figure 6 are for control surfaces with an external overhang such as a blunt-nose or Frise overhang. For shrouded overhangs such as the internal balance, the value of c_b/c_a should be multiplied by about 0.8 before using figure 6.

If the wind-tunnel data are obtained in low-speed wind tunnels, the estimated values of C_{l_p} and $\left(\alpha_p\right)_{C_h}$ should be determined for the wind-tunnel Mach number

(assume $M \doteq 0$). Otherwise the tunnel data must be corrected for compressibility effects and present methods of correcting tunnel data for compressibility are believed unsatisfactory.

ILLUSTRATIVE EXAMPLE

Stick forces are computed from the results of the wind-tunnel tests of the 0.40-scale semispan model of the wing of the same typical fighter airplane used as an illustrative example in reference 2. Because the wind-tunnel data were obtained at low speed, no corrections were applied for compressibility effects. Because this example is for illustrative purposes only, no computations were made to determine the effects of yawing motion or wing twist on the rate of roll but an empirical reduction factor was used to take account of these effects.

A drawing of the plan form of the wing of the model is presented in figure 7. The computations are made at an indicated airspeed of 250 miles per hour, which corresponds to a lift coefficient of 0.170 and to an angle of attack of 1.3°. The data required for the computations are as follows:

Scale of model	0.40
Aileron span, b_a, feet	3.07
Aileron root-mean-square chord $\bar{c}_a$, feet	0.371
Trailing-edge angle, ϕ, degrees	13.5
Slope of section lift curve, a_o, per degree	0.094
Balance-aileron-chord ratio, c_b/c_a	0.4
Aileron-chord ratio, c_a/c, (constant)	0.155
Location of inboard aileron tip, $\frac{y_1}{b/2}$	0.58
Location of outboard aileron tip, $\frac{y_o}{b/2}$	0.98
Wing aspect ratio, A	5.55
Wing taper ratio, λ	0.60
Maximum aileron deflection, $\delta_{a_{max}}$, degrees	±16
Maximum stick deflection, $\theta_{s_{max}}$, degrees	±21
Stick length, feet	2.00
Aileron-linkage-system ratio	1:1
Wing loading of airplane, W/S, pounds per square foot	27.2

The required wind-tunnel test results include rolling-moment coefficients and hinge-moment coefficients corrected for the effects of the jet boundaries. Typical data plotted against aileron deflection are presented in figure 8. These same coefficients cross-plotted against angle of attack for one-fourth, one-half, three-fourths, and full aileron deflections are given in figure 9. The value of C_{l_p}/a_o as determined from figure 2 is 4.02 and the value of C_{l_p} is 0.378. The value of $(\alpha_p)_{C_{h_{LL}}} \frac{A_c + 4}{A_c + 2} \frac{A_c E_c + 2}{A_c E'_c + 4}$ used in equation (2) to determine $(\Delta\alpha)_{C_h}$ is found from figures 3 and 4 to be 0.565 and is used to compute both the rate of roll and the stick force.

In order to facilitate the computations, simultaneous plots of C_l and $(\Delta\alpha)_{C_h}$ against $pb/2V$ were made (fig. 10).

The steps in the computation will be explained in detail for the single case of equal up and down aileron deflections of 4°:

(1) From figure 9, the values of C_l corresponding to $\delta_a = 4°$ and $\delta_a = -4°$ at $\alpha = 1.3°$ are 0.0058 and -0.0052, respectively, or a total static C_l of 0.0110.

(2) A first approximation to $(\Delta\alpha)_{C_h}$ taken at the value of $pb/2V$ corresponding to $C_l = 0.0110$ in figure 10 is found to be 0.95°.

(3) Second-approximation values of C_l (fig. 9) are determined at $\alpha = 0.35°$ for $\delta_a = 4°$ and at $\alpha = 2.25°$ for $\delta_a = -4°$, which give a total C_l of 0.0112.

(4) The second approximation to $(\Delta\alpha)_{C_h}$ is now found from figure 10 to be 0.96°, which is sufficiently close to the value found in step (2) to make any additional approximations unnecessary.

(5) By use of the value of C_l from step (3), the value of $\frac{pb}{2V} = 0.0300$ is obtained from figure 10.

(6) From figure 9 the hinge-moment coefficient corresponding to $\delta_a = 4^\circ$ and the corrected angle of attack $\alpha = 0.34^\circ$ is -0.0038 and for $\delta_a = -4^\circ$ and $\alpha = 2.26^\circ$ is 0.0052. The total C_h is therefore 0.0090.

(7) The stick force in pounds is calculated from the aileron-linkage-system data, the aileron dimensions, the increment of hinge-moment coefficient, and the lift coefficient as follows:

Stick force × Travel = Hinge moment × Deflection

where the hinge moment is equal to $C_h q b_a \bar{c}_a^2$ and the motion is linear.

Substitution of the appropriate values in the equation gives

$$F_s \frac{2 \times 21}{57.3} = \frac{16}{57.3} C_h q b_a \bar{c}_a^2$$

and the wing loading is

$$\frac{W}{S} = qC_L$$
$$= 27.2$$

Therefore,

$$F_s = \frac{27.2}{C_L} C_h \frac{3.07}{0.4} \left(\frac{0.371}{0.4}\right)^2 \frac{16 \times 57.3}{2 \times 21 \times 57.3}$$

or

$$F_s = 68.4 \frac{C_h}{C_L}$$

Thus, when $C_h = 0.0090$ and $C_L = 0.170$,

$$F_s = 68.4 \times \frac{0.0090}{0.170}$$
$$= 3.62 \text{ pounds}$$

This stick-force is that due to aileron deflection and has been corrected by $(\alpha_p)_{C_{h_{EV}}}$ as determined with the Jones edge-velocity correction applied to the lifting-line-theory value.

(8) The small additional lifting-surface correction to the hinge moment (fig. 5) is obtained from

$$\Delta(C_{h_p})_{LS} \frac{(c_a/c)^2}{F\eta} = 0.0207$$

and since $\phi = 13.50$,

$$\eta = 1 - 0.0006(13.5)^2$$
$$= 0.91$$

From figure 6,

$$\frac{F}{(c_a/c)^2} = 0.55$$

Therefore,

$$\Delta(C_{h_p})_{LS} = 0.0207 \times 0.91 \times 0.55$$
$$= 0.0103$$

and

$$\Delta(C_h)_{LS} = 0.0103 \times 0.03$$
$$= 0.0003$$

(9) The ΔF_s due to the additional lifting-surface correction of step (8) may be expressed as

$$\Delta F_s = \frac{68.4}{0.170} \Delta(C_h)_{LS}$$
$$= 0.134 \text{ pound}$$

Then,

$$\text{Total stick force} = F_s + \Delta F_s$$

$$= 3.62 + 0.124$$

$$= 3.74$$

The stick-force computations for a range of aileron deflection are presented in table I. The final stick-force curves are presented in figure 11 as a function of the value of $pb/2V$ calculated for the rigid unyawed wing. For comparison, the stick forces (first-approximation values of table I) calculated by neglecting the effect of rolling are also presented. Stick-force characteristics estimated for the flexible airplane with fixed rudder are presented in figure 11. The values of $pb/2V$ obtained for the rigid unyawed wing were simply reduced by applying an empirical factor of 0.75 as indicated by the approximate rule suggested in the preceding section. No calculations of actual wing twist or yaw and yawing motion were made for this example.

II - D E V E L O P M E N T O F M E T H O D

The method for determining values of C_{l_p} and C_{h_p} is based on the theoretical flow around a wing in steady roll with the introduction of certain empirical factors to take account of viscosity, wing twist, and minor effects. The theoretical solution is obtained by means of an electromagnetic-analogy model of the lifting surface, which simulates the wing and its wake by current-carrying conductors in such a manner that the surrounding magnetic field corresponds to the velocity field about the wing. The electromagnetic-analogy method of obtaining solutions of lifting-surface-theory problems is discussed in detail in reference 4. The present calculations were limited to the case of a thin elliptic wing of aspect ratio 6 rolling at zero angle of attack.

ELECTROMAGNETIC-ANALOGY MODEL

Vortex Pattern

In order to construct an electromagnetic-analogy model of the rolling wing and wake, it is necessary to determine first the vortex pattern that is to represent the rolling wing. The desired vortex pattern is the pattern calculated by means of the two-dimensional theories - thin-airfoil theory and lifting-line theory. The additional aspect-ratio corrections are estimated by determining the difference between the actual shape of the wing and the shape that would be required to sustain the lift distribution or vortex pattern determined from the two-dimensional theories.

For the special cases of a thin elliptic wing at a uniform angle of attack or in a steady roll, the lifting-line-theory values of the span load distribution may be obtained by means of simple calculations (reference 6). The span load distributions for both cases are equal to the span load distributions determined from strip theory with a uniform reduction in all ordinates of the span-load curves by an aerodynamic-induction factor. This factor is $\frac{A}{A + 2}$ for the wing at a uniform angle of attack and $\frac{A}{A + 4}$ for the wing in steady roll. The equation for the load at any spanwise station $\frac{y}{b/2}$ of a thin elliptic wing at zero angle of attack rolling steadily with unit wing-tip helix angle $pb/2V$ is therefore (see fig. 12)

$$\frac{cc_l}{c_s(pb/2V)} = \frac{2\pi A}{A + 4}\left(\frac{y}{b/2}\right)\sqrt{1 - \left(\frac{y}{b/2}\right)^2} \qquad (3)$$

Where $a_o = 2\pi$.

The chordwise circulation function $\frac{2\Gamma}{cc_l V}$ from thin-airfoil theory for an inclined flat plate is

$$\frac{2\Gamma}{cc_l V} = \frac{1}{\pi}\left[2\sqrt{\frac{x}{c} - \left(\frac{x}{c}\right)^2} + \cos^{-1}\left(1 - \frac{2x}{c}\right)\right] \qquad (4)$$

where x/c is measured from the leading edge. (See fig. 13 for values of $\frac{2\Gamma}{cc_l V}$.)

The vortex pattern is determined from lifting-line theory as the product of the spanwise-loading function $\frac{cc_l}{c_s(pb/2V)}$ and the chordwise circulation function $\frac{2\Gamma}{cc_l V}$ for all points on the wing and in the wake; thus,

$$\frac{2\Gamma}{c_s V(pb/2V)} = \frac{cc_l}{c_s(pb/2V)} \frac{2\Gamma}{cc_l V}$$

Contour lines of this product determine the equivalent vortex pattern of the rolling wing. Ten of these lines are shown in figure 14. The contour lines are given in terms of the parameter

$$\frac{\frac{2\Gamma}{c_s V(pb/2V)}}{\left[\frac{2\Gamma}{c_s V(pb/2V)}\right]_{max}}$$

which reduces to $\frac{\Gamma}{\Gamma_{max}}$.

Construction of the Model

Details of the construction of the model may be seen from the photographs of figure 1. The tests were made under very nearly the same conditions as were the tests of the preliminary electromagnetic-analogy model reported in reference 4. The span of the model was

twice that of the model of reference 4 (6.56 ft instead of 3.28 ft), but since the aspect ratio is twice as large (6 instead of 3), the maximum chord is the same.

In order to simplify the construction of the model, only one semispan of the vortex sheet was simulated. Also, in order to avoid the large concentrations of wires at the leading edge and tips of the wing, this semispan of the vortex sheet was constructed of two sets of wires; each of the wires in the set representing the region of high load grading simulated a larger increment of $\Delta\left(\frac{\Gamma}{\Gamma_{max}}\right)$ than the wires in the set representing the region of low load grading.

Downwash Measurements

The magnetic-field strength was measured at 4 or 5 vertical heights, 15 spanwise locations, and 25 to 50 chordwise stations. A number of repeat tests were made to check the accuracy of the measurements and satisfactory checks were obtained.

The electric current was run through each set of wires separately. With the current flowing through one set of wires, readings were taken at points on the model and at the reflection points and the sum of these readings was multiplied by a constant determined from the increment of vorticity $\Delta\left(\frac{\Gamma}{\Gamma_{max}}\right)$ represented by that set of wires. Then, with the current flowing through the other set of wires, readings were taken at both real and reflection points and the sum of these readings was multiplied by the appropriate constant. The induced downwash was thus estimated from the total of the four readings. The fact that four separate readings had to be added together did not result in any particular loss in accuracy, because readings at the missing semispan were fairly small and less influenced by local effects of the incremental vortices. A more accurate vortex distribution was made possible by using two separate sets of wires. The measured data were faired, extrapolated to zero vertical height, and converted to the downwash function $\frac{wb}{2\Gamma_{max}}$ as discussed in reference 4. The final curves of $\frac{wb}{2\Gamma_{max}}$ are

presented for the quarter chord, half chord, and three-quarter chord in figure 15. Also presented in figure 15 are values of $\frac{wb}{2\Gamma_{max}}$ calculated by lifting-line theory and values calculated by lifting-line theory as corrected by the Jones edge-velocity correction.

DEVELOPMENT OF FORMULAS

General Discussion

Lifting-surface corrections.- The measurements of the magnetic-field strength (induced downwash) of the electromagnetic-analogy model of the rolling wing give the shape of the surface required to support the distribution of lift obtained by lifting-line theory. Corrections to the spanwise and chordwise load distributions may be determined from the difference between the assumed shape of the surface and the shape indicated by the downwash measurements. Formulas for determining these corrections to the span load distributions and the rolling- and hinge-moment characteristics have been developed in connection with jet-boundary-correction problems (reference 5). These formulas are based on the assumption that the difference between the two surfaces is equivalent at each section to an increment of angle of attack plus an increment of circular camber. From figure 15 it may be seen that such assumptions are justified since the chordwise distribution of downwash is approximately linear. It should be noted that these formulas are based on thin-airfoil theory and thus do not take into account the effects of viscosity, wing thickness, or compressibility.

Viscosity.- The complete additional aspect-ratio correction consists of two parts. The main part results from the streamline curvature and the other part results from an additional increment of induced angle of attack (the angle at the 0.5c point) not determined by lifting-line theory. The second part of the correction is normally small, 5 to 10 percent of the first part of the correction. Some experimental data indicate that the effect of viscosity and wing thickness is to reduce the theoretical streamline-curvature correction by about 10 percent for airfoils with small trailing-edge angles.

Essentially the same final answer is therefore obtained whether the corrections are applied in two parts (as should be done, strictly speaking) or whether they are applied in one part by use of the full theoretical value of the streamline-curvature correction. The added simplicity of using a single correction rather than applying it in two parts led to the use of the method of application of reference 3.

The use of the single correction worked very well for the ailerons of reference 3, which were ailerons with small trailing-edge angles. A study is in progress at the Langley Laboratories of the NACA to determine the proper aspect-ratio corrections for ailerons and tail surfaces with beveled trailing edges. For beveled trailing edges, in which viscous effects may be much more pronounced than in ailerons with small trailing-edge angles, the reduction in the theoretical streamline-curvature correction may be considerably more than 10 percent; also, when C_{h_α} is positive, the effects of the reduction in the streamline-curvature correction and the additional downwash at the 0.50c point are additive rather than compensating. Although at present insufficient data are available to determine accurately the magnitude of the reduction in the streamline-curvature correction for beveled ailerons, it appears that the simplification of applying aspect-ratio corrections in a single step is not allowable for beveled ailerons. The corrections will therefore be determined in two separate parts in order to keep them general: one part, a streamline-curvature correction and the other, an angle-of-attack correction. An examination of the experimental data available indicates that more accurate values of the hinge moment resulting from streamline curvature are obtained by multiplying the theoretical values by an empirical reduction factor η which is approximately equal to $1 - 0.0005\phi^2$ where ϕ is the trailing-edge angle in degrees. This factor will doubtless be modified when further experimental data are available.

Compressibility.- The effects of compressibility upon the additional aspect-ratio corrections were not considered in reference 3. First-order compressibility effects can be accounted for by application of the Prandtl-Glauert rule to lifting-surface-theory results. (See reference 7.) This method consists in

determining the compressible-flow characteristics of an equivalent wing, the chord of which is increased by the ratio $\frac{1}{\sqrt{1 - M^2}}$ where M is the ratio of the free-stream velocity to the velocity of sound. Because approximate methods of extrapolating the estimated hinge-moment and damping-moment parameters to wings of any aspect ratio will be determined, it is necessary to estimate only the hinge-moment and damping parameters corresponding to an equivalent wing with its aspect ratio decreased by the ratio $\sqrt{1 - M^2}$. The estimated parameters for the equivalent wing are then increased by the ratio $\frac{1}{\sqrt{1 - M^2}}$.

The formulas presented subsequently in the section "Approximate Method of Extending Results to Wings of Other Aspect Ratios" are developed for $M = 0$, but the figures are prepared by substituting $A_c = A\sqrt{1 - M^2}$ for A and multiplying the parameters as plotted by $\sqrt{1 - M^2}$. The edge-velocity correction factors E_c, E_{ec}, E'_c, and E'_{ec} are the factors corresponding to A_c. The figures thus include corrections for first-order compressibility effects.

Thin Elliptic Wing of Aspect Ratio 6

Damping in roll C_{l_p}.- In order to calculate the correction to the lifting-line-theory values of the damping derivative C_{l_p} it is necessary to calculate the rolling moment that would result from an angle-of-attack distribution along the wing span equal to the difference between the measured downwash (determined by the electromagnetic-analogy method) at the three-quarter-chord line and the downwash values given by lifting-line theory. (See fig. 15.)

Jones has obtained a simple correction to the lifting-line-theory values of the lift (reference 1) and the damping in roll (unpublished data) for flat

elliptic wings. This correction, termed the "Jones edge-velocity correction," is applied by multiplying the lifting-line-theory values of the lift by the ratio $\frac{A_c + 2}{A_c E_c + 2}$ and the lifting-line-theory values of the damping in roll by $\frac{A_c + 4}{A_c E'_c + 4}$ with values of E_c and E'_c as given in figure 16. As may be seen from figure 15, the downwash given by the Jones edge-velocity correction is almost exactly that measured at the 0.50c points for flat elliptic wings. This fact is useful in estimating the lifting-surface corrections because the edge-velocity correction, which is given by a simple formula, can be used to correct for the additional angle of attack indicated by the linear difference in downwash at the 0.50c line.

The variation in downwash between the 0.25c line and 0.75c line, apparently linear along the chord, indicates an approximately circular streamline curvature or camber of the surface. The increment of lift resulting at each section from circular camber is equal to that caused by an additional angle of attack given by the slope of the section at 0.75c relative to the chord line or the tangent at 0.50c - that is, $\left(\frac{w}{V}\right)_{0.75c} - \left(\frac{w}{V}\right)_{0.50c}$. Because this difference in downwash does not vary linearly along the span, a spanwise integration is necessary to determine the streamline-curvature increment in rolling moment; that is,

$$\left(\Delta C_l\right)_{SC} = \frac{8\Gamma_{max} A_c}{bV\left(A_c E'_c + 4\right)} \int_0^1 \left[\left(\frac{wb}{2\Gamma_{max}}\right)_{0.75c} - \left(\frac{wb}{2\Gamma_{max}}\right)_{0.50c}\right] \frac{c}{c_s} \frac{y}{b/2} \, d\left(\frac{y}{b/2}\right) \qquad (5)$$

An evaluation of Γ_{max} in terms of $pb/2V$ is necessary to determine the correction to the damping-moment coefficient C_{l_p}. The lifting-line-theory relation

between Γ_{max} and $pb/2V$ is, from equation (3),

$$\Gamma_{max} = \frac{2Vb(pb/2V)}{A + 4}$$

With the edge-velocity correction applied

$$\Gamma_{max} = \frac{2Vb(pb/2V)}{A_c E'_c + 4} \tag{6}$$

The value of the streamline-curvature correction to C_{l_p} is therefore

$$\left(\Delta C_{l_p}\right)_{SC} = \frac{16A_c}{(A_c E'_c + 4)^2} \int_0^1 \left[\left(\frac{wb}{2\Gamma_{max}}\right)_{0.75c} - \left(\frac{wb}{2\Gamma_{max}}\right)_{0.50c}\right] \frac{c}{c_s} \frac{y}{b/2} d\left(\frac{y}{b/2}\right) \tag{7}$$

A graphical integration of equation (7) gives a value of 0.022 for $\left(\Delta C_{l_p}\right)_{SC}$.

By the integration of equation (3), the value of $\left(C_{l_p}\right)_{LL}$ for incompressible flow is found to be $\frac{\pi}{4} \frac{A}{A + 4} = 0.471$ for $A = 6$.

Application of the edge-velocity correction, for $A = 6$, gives

$$\left(C_{l_p}\right)_{EV} = \frac{\pi A}{4(AE' + 4)}$$
$$= 0.433$$

and, finally, subtracting the streamline-curvature correction gives a value of C_{l_p}, for $A = 6$, as follows:

$$C_{l_p} = \left(C_{l_p}\right)_{EV} - \left(\Delta C_{l_p}\right)_{SC}$$
$$= 0.411$$

The value of C_{l_p} for a wing of aspect ratio 6 is therefore 13 percent less than the value given by lifting-line theory and 5 percent less than that given by lifting-line theory with the Jones edge-velocity correction applied.

Hinge-moment parameter C_{h_p}.- The streamline-curvature correction to C_{h_p} for constant-percentage-chord ailerons is, from reference 5 and with the value of Γ_{max} given in equation (6),

$$\left(\Delta C_{h_p}\right)_{SC} = \frac{2F\eta \int \left[\frac{\partial\left(wb/2\Gamma_{max}\right)}{\partial(x/c)}\right]\left(\frac{c}{c_s}\right)^2 d\left(\frac{y}{b/2}\right)}{\left(\frac{c_a}{c}\right)^2 \left(A_c E'_c + 4\right) \int \left(\frac{c}{c_s}\right)^2 d\left(\frac{y}{b/2}\right)} \qquad (8)$$

where the integrations are made across the aileron span. Because the downwash at the 0.50c point is given satisfactorily by applying the edge-velocity correction to the lifting-line-theory values of the downwash, the part of the correction to C_{h_p} which depends upon the downwash at the 0.50c point may be determined by means of the edge-velocity correction. The effect of aerodynamic induction was neglected in developing equation (8) because aerodynamic induction has a very small effect upon the hinge-moment corrections caused by streamline curvature.

Values of the factor $\frac{F}{(c_a/c)^2}$ for various aileron-chord ratios and balance ratios as determined from thin-airfoil theory are given in figure 6. As mentioned previously, η is a factor that approximately accounts for the combined effects of wing thickness and viscosity in altering the calculated values of $\frac{F}{(c_a/c)^2}$. The experimental data available at present indicate that $\eta \approx 1 - 0.0005\phi^2$. Results of the integration of equation (8) for the elliptic wing of aspect ratio 6 are given in figure 17 as the parameter $\left(\Delta C_{h_p}\right)_{SC} \frac{(c_a/c)^2}{F\eta}\left(A_c + 1\right)\sqrt{1 - M^2}$. Values

of $\left(\Delta C_{h_\alpha}\right)_{SC} \frac{\left(c_a/c\right)^2}{F\eta} \left(A_c + 1\right) \sqrt{1 - M^2}$ determined as in reference 3 are given in figure 18.

The value of $\left(C_{h_p}\right)_{LS}$ is

$$\left(C_{h_p}\right)_{LS} = \left(C_{h_\alpha}\right)_{LL} \left(\alpha_p\right)_{C_{h_{LL}}} \frac{A_c + 4}{A_c E'_c + 4} + \left(\Delta C_{h_p}\right)_{SC}$$

Since

$$\frac{A_c + 2}{A_c E_c + 2} \left(C_{h_\alpha}\right)_{LL} = \left(C_{h_\alpha}\right)_{LS} - \left(\Delta C_{h_\alpha}\right)_{SC}$$

then

$$\left(C_{h_p}\right)_{LS} = \left(\alpha_p\right)_{C_{h_{LL}}} \frac{A_c + 4}{A_c E'_c + 4} \frac{A_c E_c + 2}{A_c + 2} \left(C_{h_\alpha}\right)_{LS}$$

$$+ \left(\Delta C_{h_p}\right)_{SC} - \left(\Delta C_{h_\alpha}\right)_{SC} \left(\alpha_p\right)_{C_{h_{LL}}} \frac{A_c + 4}{A_c E'_c + 4} \frac{A_c E_c + 2}{A_c + 2}$$

or

$$\left(C_{h_p}\right)_{LS} = \left[\left(\alpha_p\right)_{C_{h_{EV}}} \left(C_{h_\alpha}\right)_{LS}\right] + \left[\Delta\left(C_{h_p}\right)_{LS}\right] \qquad (9)$$

The formula for the parameter $\left(\alpha_p\right)_{C_{h_{LL}}}$ is derived for elliptic wings in the appendix, and numerical values are given in the form $\left(\alpha_p\right)_{C_{h_{LL}}} \frac{A_c + 4}{A_c + 2}$ in figure 3, together with values for tapered wings derived from the data of reference 2.

It may be noted that use of the parameter $\left(\alpha_p\right)_{C_{h_{LS}}}$ to determine the total correction for rolling would be impractical because $\left(C_{h_p}\right)_{LS}$ is not proportional

to $\left(C_{h_\alpha}\right)_{LS}$. Although the numerical values of $\left(\alpha_p\right)_{Ch_{LS}}$ vary considerably with $\left(C_{h_\alpha}\right)_{LS}$, the actual effect on the stick forces is small because $\left(\alpha_p\right)_{Ch_{LS}}$ changes most with $\left(C_{h_\alpha}\right)_{LS}$ when the values of $\left(C_{h_\alpha}\right)_{LS}$ are small. This effect is illustrated in figure 19, in which numerical values of $\left(\alpha_p\right)_{Ch_{LS}}$ for a thin elliptic wing of aspect ratio 6 are given, together with the values obtained by lifting-line theory, the values obtained by applying the Jones edge-velocity correction, and the values obtained by using the aileron midpoint rule (reference 8). The values obtained by the use of the Jones edge-velocity correction are shown to be 4.4 percent less than those obtained by the use of lifting-line theory.

The right-hand side of equation (9) is divided into the following two parts:

$$\text{Part I} = \left(\alpha_p\right)_{Ch_{EV}} \left(C_{h_\alpha}\right)_{LS}$$

$$\text{Part II} = \Delta\left(C_{h_p}\right)_{LS}$$

Part I of the correction for rolling can be applied to the static hinge-moment data as a change in the effective angle of attack as in reference 2. (Also see equation (2).) Part II of equation (9), however, is applied directly as a change in the hinge-moment coefficients,

$$\Delta C_h = \Delta\left(C_{h_p}\right)_{LS} \frac{pb}{2V}$$

Inasmuch as part II of equation (9) is numerically fairly small $\left(\Delta C_h \approx 0.002 \text{ for } \frac{pb}{2V} = 0.1 \text{ for a wing of aspect ratio 6}\right)$, it need not be applied at all except for fairly large airplanes at high speed.

Approximate Method of Extending Results to Wings of Other Aspect Ratios

Damping in roll C_{l_p}.- In order to make the results of practical value, it is necessary to formulate at least approximate rules for extending the results for a thin elliptic wing of aspect ratio 6 to wings of other aspect ratios. There are lifting-surface-theory solutions (references 4 and 9) for thin elliptic wings of $A = 3$ and $A = 6$ at a uniform angle of attack. The additional aspect-ratio correction to C_{L_α} was computed for these cases and was found to be approximately one-third greater for each aspect ratio than the additional aspect-ratio correction estimated from the Jones edge-velocity correction.

The additional aspect-ratio correction to C_{l_p} for the electromagnetic-analogy model of $A = 6$ was also found to be about one-third greater than the corresponding edge-velocity correction to C_{l_p}. A reasonable method of extrapolating the values of C_{l_p} to other aspect ratios, therefore, is to use the variation of the edge-velocity correction with aspect ratio as a basis from which to work and to increase the magnitude by the amount required to give the proper value of C_{l_p} for $A = 6$. Effective values of E and E' $\left(E_e \text{ and } E'_e\right)$ were thus obtained that would give the correct values of C_{L_α} for $A = 3$ and $A = 6$ and of C_{l_p} for $A = 6$. The formulas used for estimating E_{e_c} and E'_{e_c} for other aspect ratios were

$$E_{e_c} = 1.65\left(E_c - 1\right) + 1$$

$$E'_{e_c} = 1.65\left(E'_c - 1\right) + 1$$

Values of E_{e_c} and E'_{e_c} are given in figure 16.

Values of $\frac{C_{l_p}}{a_o}\sqrt{1 - M^2}$ determined by using E'_{e_c} are presented in figure 2 as a function of A_c/a_o

where $A_c = A\sqrt{1 - M^2}$ and a_o is the incompressible slope of the section lift curve per degree.

Hinge-moment parameter C_{h_p}.- In order to determine C_{h_p} for other aspect ratios, it is necessary to estimate the formulas for extrapolating the streamline-curvature corrections $\left(\Delta C_{h_\alpha}\right)_{SC}$ and $\left(\Delta C_{h_p}\right)_{SC}$. Values of $\left(\Delta C_{h_\alpha}\right)_{SC}$ for $A = 3$ and $A = 6$ are available in reference 3. Values of $\left(\Delta C_{h_\alpha}\right)_{SC}$ might be expected to be approximately inversely proportional to aspect ratio and an extrapolation formula in the form $\left(\Delta C_{h_\alpha}\right)_{SC} = \frac{K_1}{A + K_2}$ is therefore considered satisfactory. The values of K_1 and K_2 are determined so that the values of $\left(\Delta C_{h_\alpha}\right)_{SC}$ for $A = 3$ and $A = 6$ are correct. Values of K_1 and K_2 vary with aileron span. The values of K_2, however, for all aileron spans less than 0.6 of the semispan are fairly close to 1.0; thus, by assuming a constant value of $K_2 = 1.0$ for all aileron spans and calculating values of K_1, a satisfactory extrapolation formula may be obtained. It is impossible to determine such a formula for $\left(\Delta C_{h_p}\right)_{SC}$ because results are available only for $A = 6$; however, it seems reasonable to assume the same form for the extrapolation formula and to use the same value of K_2 as for $\left(\Delta C_{h_\alpha}\right)_{SC}$. The value of K_1 can, of course, be determined from the results for $A = 6$.

Although no proof is offered that these extrapolation formulas are accurate, they are applied only to part II of equation (9) $\left(\text{values of } \Delta\left(C_{h_p}\right)_{LS}\right)$, which is numerically quite small, and are therefore considered justified.

CONCLUDING REMARKS

From the results of tests made on an electromagnetic-analogy model simulating a thin elliptic wing of aspect ratio 6 in a steady roll, lifting-surface-theory values of the aspect-ratio corrections for the damping in roll and aileron hinge moments for a wing in steady roll were obtained that are considerably more accurate than those given by lifting-line theory. First-order effects of compressibility were included in the computations.

It was found that the damping in roll obtained by lifting-surface theory for a wing of aspect ratio 6 is 13 percent less than that given by lifting-line theory and 5 percent less than that given by the lifting-line theory with the Jones edge-velocity correction applied. The results are extended to wings of any aspect ratio.

In order to estimate aileron stick forces from static wind-tunnel data, it is necessary to know the relation between the rate of change of hinge moments with rate of roll and the rate of change of hinge moments with angle of attack. It was found that this ratio is very nearly equal, within the usual accuracy of wind-tunnel measurements, to the values estimated by using the Jones edge-velocity correction, which for an aspect ratio of 6 gives values 4.4 percent less than those obtained by means of lifting-line theory. The additional lifting-surface-theory correction that was calculated need only be applied in stick-force estimations for fairly large, high-speed airplanes.

Although the method of applying the results in the general case is based on a fairly complicated theory, it may be applied rather simply and without any reference to the theoretical section of the report.

Langley Memorial Aeronautical Laboratory
National Advisory Committee for Aeronautics
Langley Field, Va.

APPENDIX

EVALUATION OF $(\alpha_p)_{Ch_{LL}}$ FOR ELLIPTIC WINGS

It was shown in reference 2 that for constant-percentage-chord ailerons the hinge moment at any aileron section is proportional to the section lift coefficient multiplied by the square of the wing chord; for constant-chord ailerons, the hinge moment at any aileron section is proportional to the section lift coefficient divided by the wing chord. The factor $(\alpha_p)_{Ch_{LL}}$ is obtained by averaging the two factors $c_l c^2$ and c_l/c across the aileron span for a rolling wing and a wing at constant angle of attack. For elliptic wings, with a slope of the section lift curve of 2π, it was shown in reference 6 that strip-theory values multiplied by aerodynamic-induction factors $\frac{A_c}{A_c + 2}$ or $\frac{A_c}{A_c + 4}$ could be used. (Note that A_c is substituted for A to account for first-order effects of compressibility.) Thus, for constant-percentage-chord ailerons on a rolling elliptic wing,

$$c_l c^2 = \frac{A_c}{A_c + 4} \sin^2\theta \; c_s{}^2 2\pi \frac{py}{V}$$

$$= \frac{2\pi c_s{}^2 A_c}{A_c + 4} \frac{pb}{2V} \sin^2\theta \cos\theta$$

and for the same wing at a constant angle of attack α

$$c_l c^2 = \frac{A_c}{A_c + 2} \sin^2\theta \; c_s{}^2 2\pi\alpha$$

In order to find $(\alpha_p)_{Ch_{LL}}$, the integral $\int c_l c^2 \, dy$ across the aileron span must be equal for both the

rolling wing and the wing at constant α. Thus,

$$\int c_l c^2 \, dy = \frac{2\pi c_s^2 A_c}{A_c + 4} \frac{pb}{2V} \int \sin^2\theta \cos\theta \, dy$$

$$= \frac{2\pi c_s^2 A_c}{A_c + 2} \alpha \int \sin^2\theta \, dy$$

$$dy = \frac{b}{2} d(\cos\theta)$$

$$= -\frac{b}{2} \sin\theta \, d\theta$$

Let

$$\alpha = \left(\alpha_p\right)_{Ch_{LL}} \frac{pb}{2V}$$

Then

$$\left(\alpha_p\right)_{Ch_{LL}} = \frac{A_c + 2}{A_c + 4} \frac{\int \sin^3\theta \cos\theta \, d\theta}{\int \sin^3\theta \, d\theta}$$

$$= \frac{A_c + 2}{A_c + 4} \frac{\frac{1}{4}\left[\sin^4\theta\right]_{\theta_1}^{\theta_o}}{\frac{1}{3}\left[\sin^2\theta \cos\theta + 2\cos\theta\right]_{\theta_1}^{\theta_o}}$$

where θ_o and θ_1 are parameters that correspond to the outboard and inboard ends of the aileron, respectively. Values of $\left(\alpha_p\right)_{Ch_{LL}} \frac{A_c + 4}{A_c + 2}$ were calculated for the outboard end of the aileron at $\frac{y}{b/2} = 0.95$ and plotted in figure 3.

A similar development gives, for the constant-chord aileron,

$$\int \frac{c_l}{c}\,dy = \frac{2\pi A_c}{c_s\left(A_c + 4\right)} \frac{pb}{2V} \int \frac{\cos\theta}{\sin\theta}\,dy$$

$$= \frac{2\pi A_c}{c_s\left(A_c + 2\right)} \frac{pb}{2V} \left(\alpha_p\right)_{Ch_{LL}} \int \frac{dy}{\sin\theta}$$

$$\left(\alpha_p\right)_{Ch_{LL}} \frac{A_c + 4}{A_c + 2} = \frac{\int \cos\theta\,d\theta}{\int d\theta}$$

$$= \frac{\left[\sin\theta\right]_{\theta_i}^{\theta_o}}{\left[\theta\right]_{\theta_i}^{\theta_o}}$$

These values are also presented in figure 3.

REFERENCES

1. Jones, Robert T.: Theoretical Correction for the Lift of Elliptic Wings. Jour. Aero. Sci., vol 9, no. 1, Nov. 1941, pp. 8-10.

2. Swanson, Robert S., and Toll, Thomas A.: Estimation of Stick Forces from Wind-Tunnel Aileron Data. NACA ARR No. 3J29, 1943.

3. Swanson, Robert S., and Gillis, Clarence L.: Limitations of Lifting-Line Theory for Estimation of Aileron Hinge-Moment Characteristics. NACA CB No. 3L02, 1943.

4. Swanson, Robert S., and Crandall, Stewart M.: An Electromagnetic-Analogy Method of Solving Lifting-Surface-Theory Problems. NACA ARR No. L5D23, 1945.

5. Swanson, Robert S., and Toll, Thomas A.: Jet-Boundary Corrections for Reflection-Plane Models in Rectangular Wind Tunnels. NACA ARR No. 3E22, 1943.

6. Munk, Max M.: Fundamentals of Fluid Dynamics for Aircraft Designers. The Ronald Press Co., 1929.

7. Goldstein, S., and Young, A. D.: The Linear Perturbation Theory of Compressible Flow with Applications to Wind-Tunnel Interference. 6865, Ae. 2262, F.M. 601, British A.R.C., July 6, 1943.

8. Harris, Thomas A.: Reduction of Hinge Moments of Airplane Control Surfaces by Tabs. NACA Rep. No. 528, 1935.

9. Cohen, Doris: A Method for Determining the Camber and Twist of a Surface to Support a Given Distribution of Lift. NACA TN No. 855, 1942.

TABLE I.- EXAMPLE OF STICK-FORCE COMPUTATIONS

[Values of C_l and C_h from fig. 9; values of pb/2V and $\Delta\alpha$ from fig. 10.]

Determination of corrections due to effect of roll					Determination of stick forces				
δ_a(deg)	±4	±8	±12	±16	δ_a(deg)	±4	±8	±12	±16
First approximation, static values									
[1]$(C_l)_{\delta_a}$	0.0058	0.0111	0.0166	0.0208	[1]$(C_h)_{\delta_a}$	-0.0038	-0.0080	-0.0145	-0.0290
[1]$(C_l)_{-\delta_a}$	-0.0052	-0.0105	-0.0157	-0.0206	[1]$(C_h)_{-\delta_a}$	0.0038	0.0112	0.0190	0.0235
C_l	0.0110	0.0216	0.0323	0.0414	C_h	0.0076	0.0192	0.0335	0.0525
[2]pb/2V	0.0295	0.0575	0.0858	0.1095	$F_s = 402\ C_h$	3.06	7.73	13.46	21.10
$(\Delta\alpha)_{C_h}$	0.95	1.86	2.78	3.55					
Second approximation									
[1]$(\alpha)_{\delta_a}$	0.35	-0.56	-1.48	-2.25	[1]$(\alpha)_{\delta_a}$	0.34	-0.61	-1.61	-2.46
[1]$(C_l)_{\delta_a}$	0.0058	0.0111	0.0169	0.0212	[1]$(C_h)_{\delta_a}$	-0.0038	-0.0060	-0.0053	-0.0062
[1]$(\alpha)_{-\delta_a}$	2.25	3.16	4.08	4.85	[1]$(\alpha)_{-\delta_a}$	2.26	3.21	4.21	5.06
[1]$(C_l)_{-\delta_a}$	-0.0054	-0.0111	-0.0170	-0.0225	[1]$(C_h)_{-\delta_a}$	0.0052	0.0137	0.0168	0.0180
C_l	0.0112	0.0222	0.0339	0.0437	C_h	0.0090	0.0197	0.0221	0.0242
[2]pb/2V	0.0300	0.0592	0.0900	0.1160	$F_s = 402\ C_h$	3.62	7.92	8.88	9.73
$(\Delta\alpha)_{C_h}$	0.96	1.91	2.91	3.76	$F_s + \Delta F_s$	3.74	8.17	9.25	10.21
0.75pb/2V	0.0225	0.0444	0.0675	0.0870					

[1]Subscripts are used to indicate positive or negative aileron deflections.

[2]These values of pb/2V are for a rigid unyawed wing.

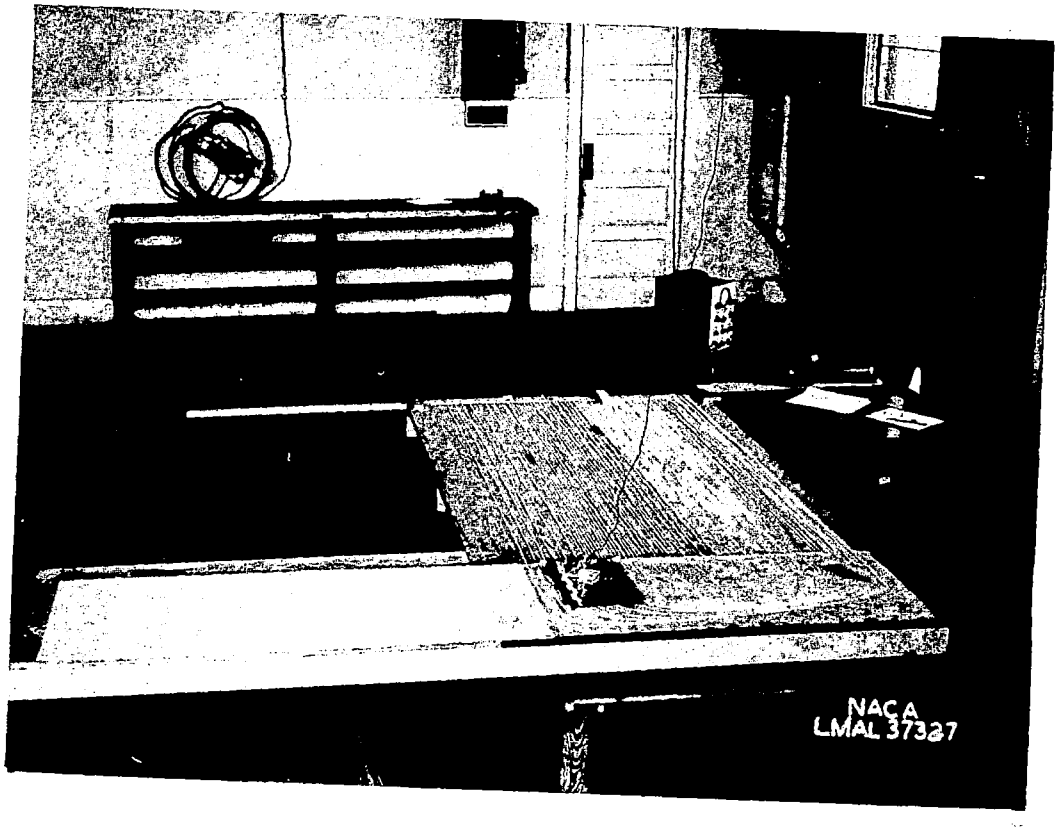

(a) General setup.

Figure 1.- Electromagnetic-analogy model simulating a semispan of a thin elliptic wing of aspect ratio 6 in a steady roll.

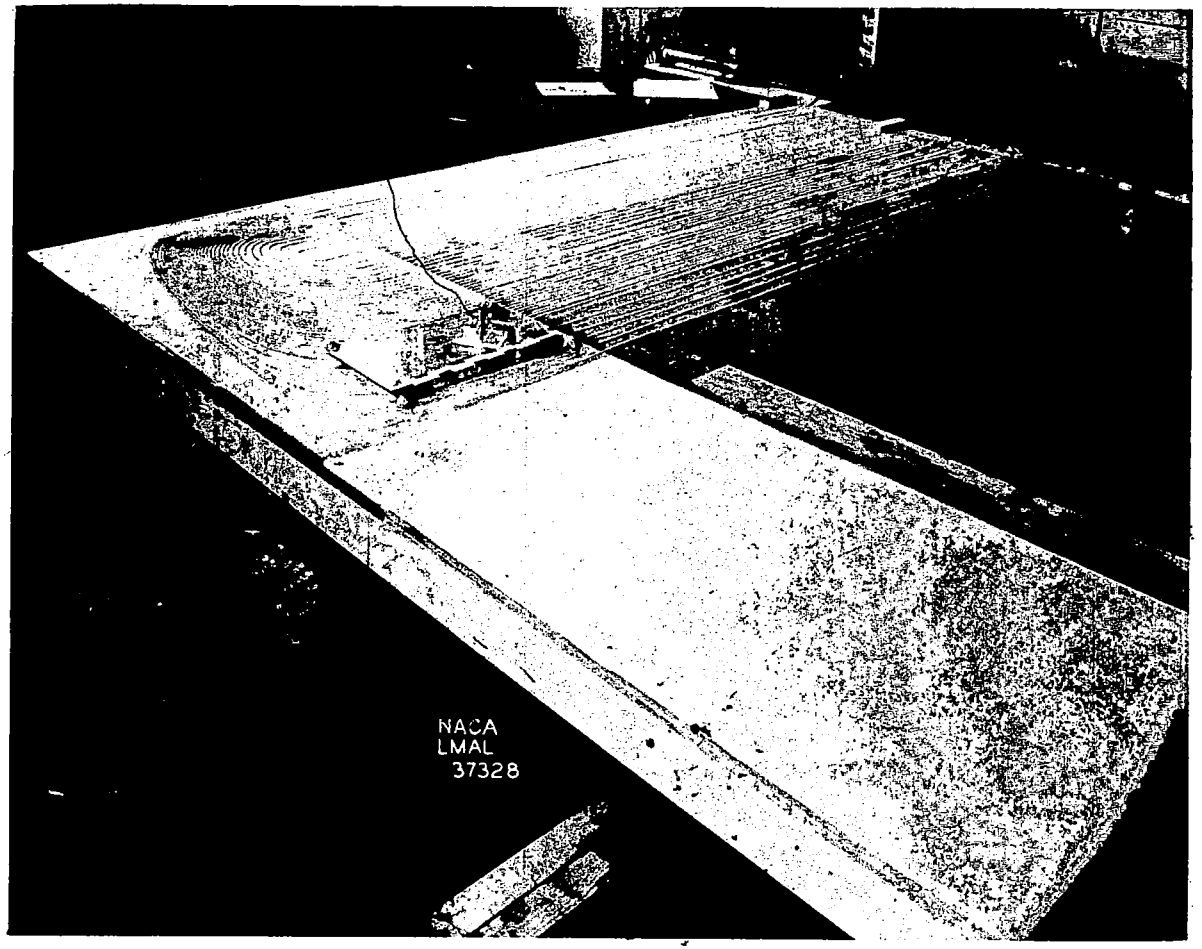

(b) Close-up showing search coil.

Figure 1.- Concluded.

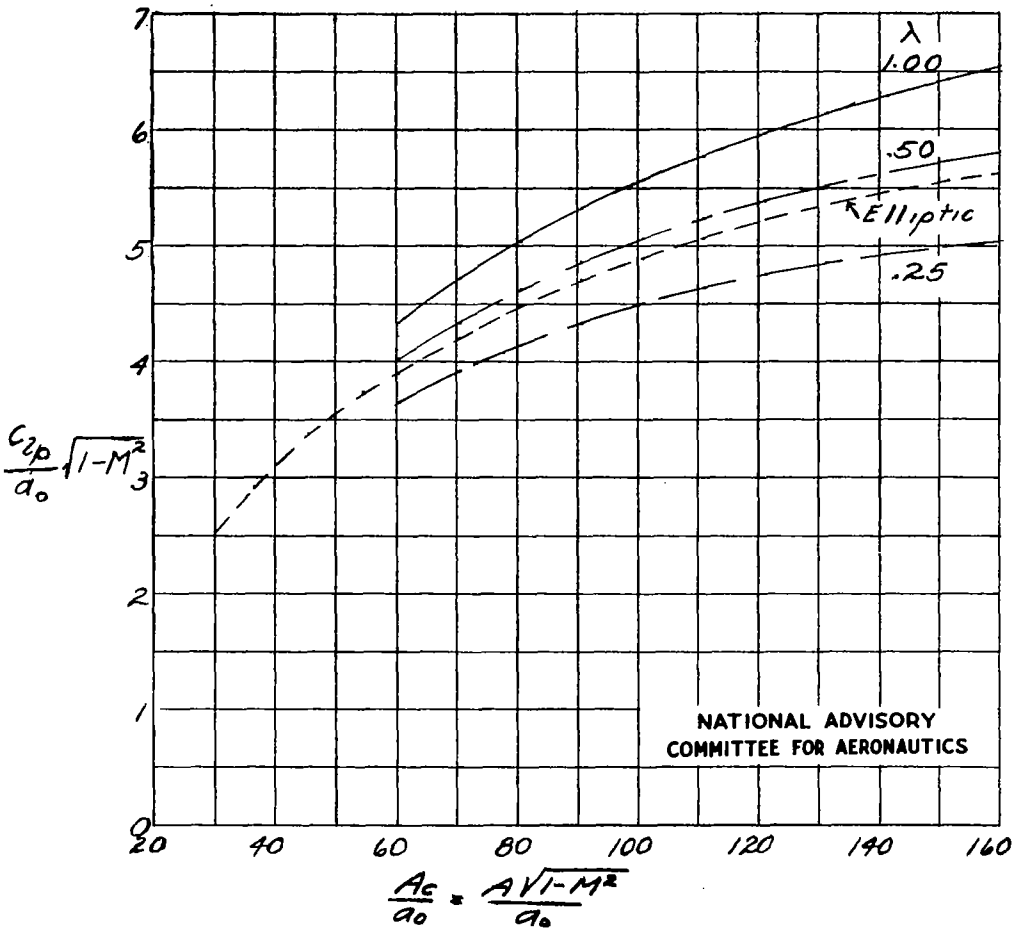

Figure 2.- Variation of damping coefficient with aspect ratio and taper ratio in terms of slope of section lift curve for incompressible flow (per degree). (Lifting-line-theory values of reference 2 with an effective edge-velocity correction applied.)

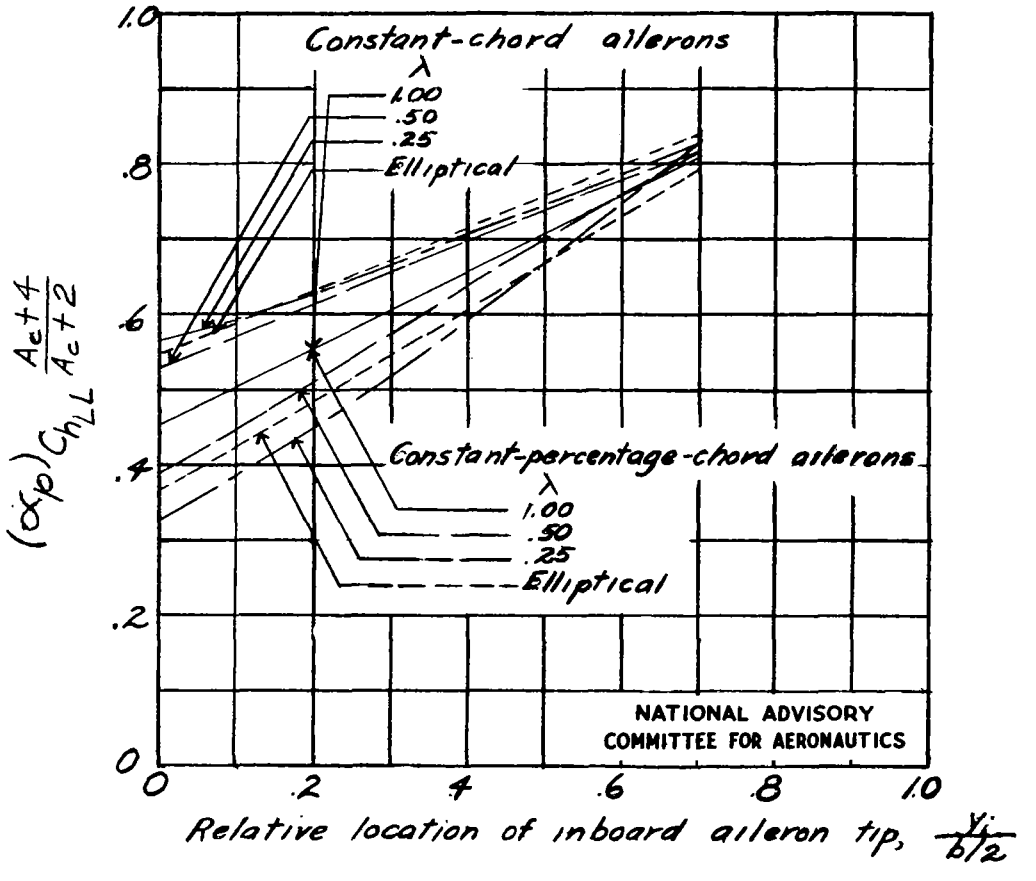

Figure 3.- Values of $(\alpha_p)_{C_{h_{LL}}} \frac{A_c + 4}{A_c + 2}$ for various aileron tip locations. The corrections of figure 4 must be used with these values.

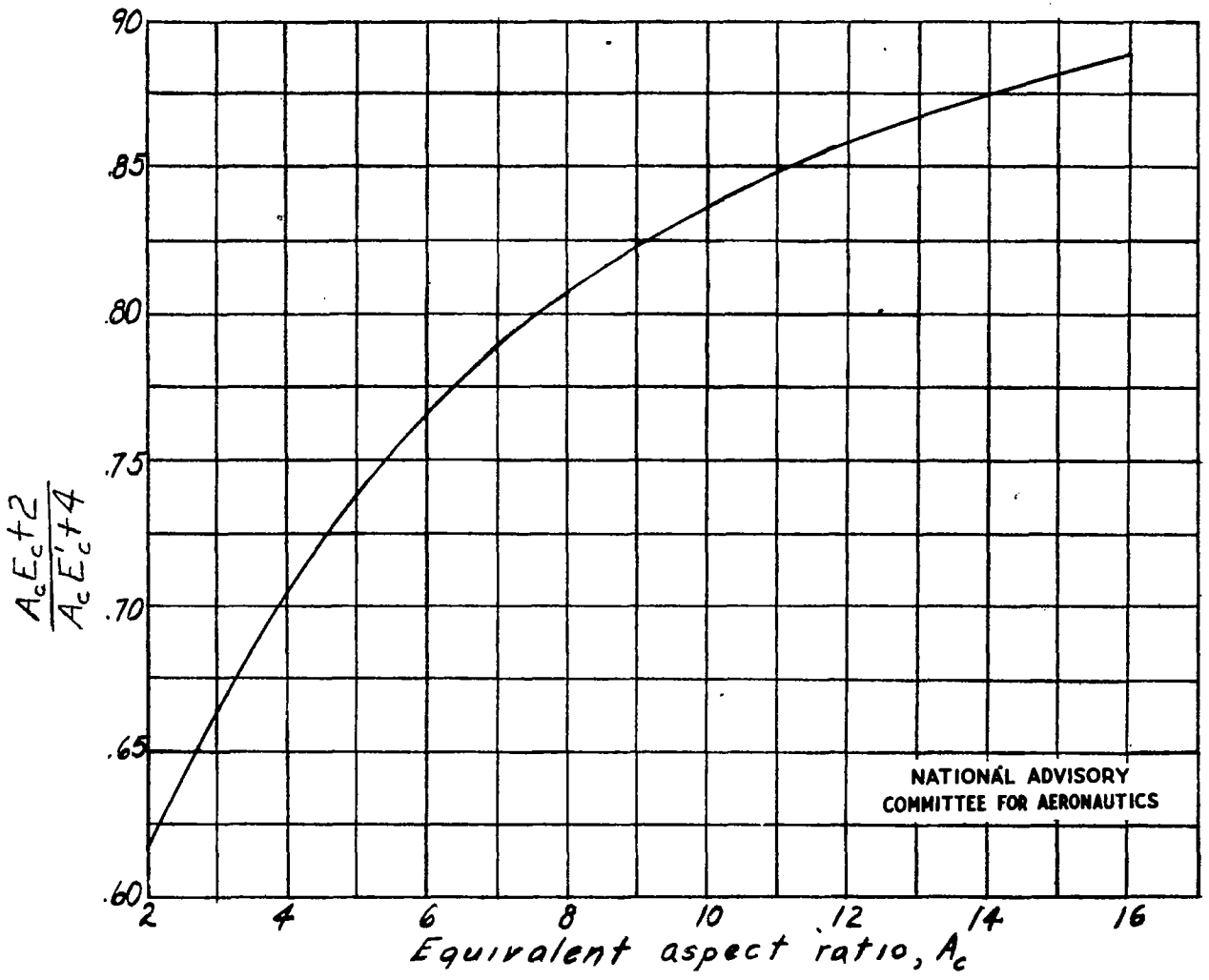

Figure 4.- Variation of $\frac{A_cE_c + 2}{A_cE'_c + 4}$ with equivalent aspect ratio.

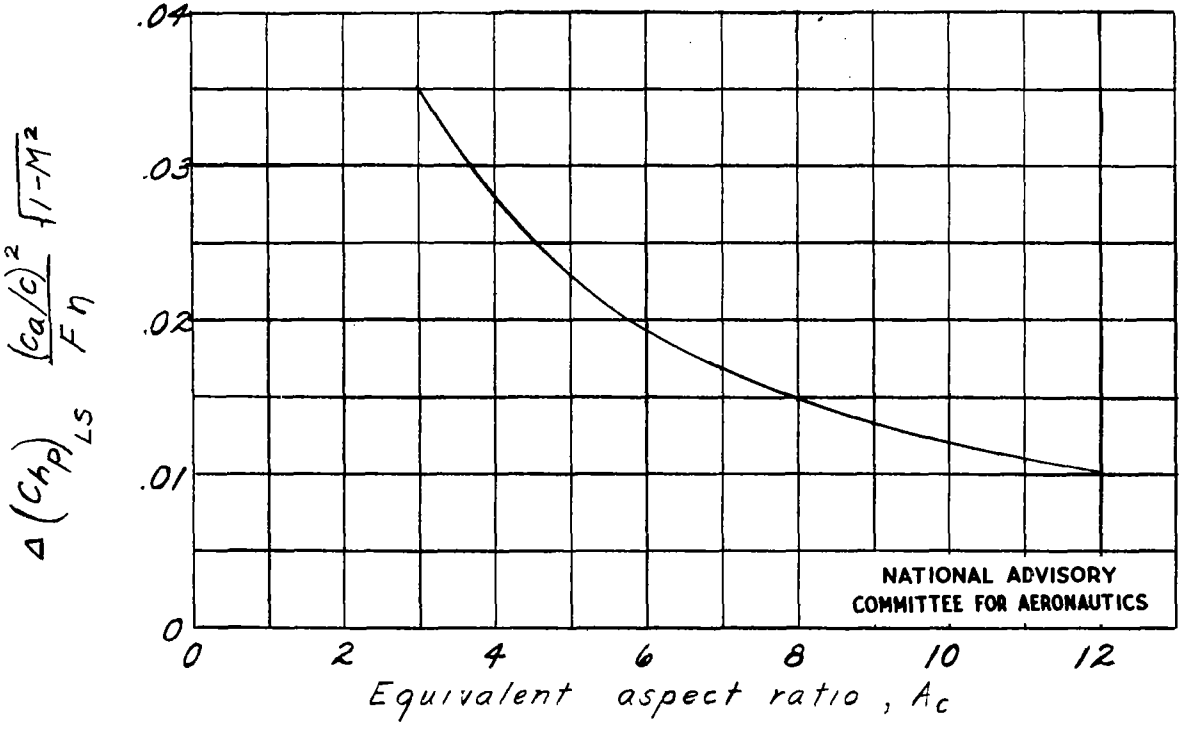

Figure 5.- Lifting-surface-correction parameter $\Delta(c_{h_p})_{LS} \frac{(c_a/c)^2}{F\eta} \sqrt{1 - M^2}$.
(For values of $\frac{(c_a/c)^2}{F}$, see fig. 6; $\eta \approx 1 - 0.0005\phi^2$.)

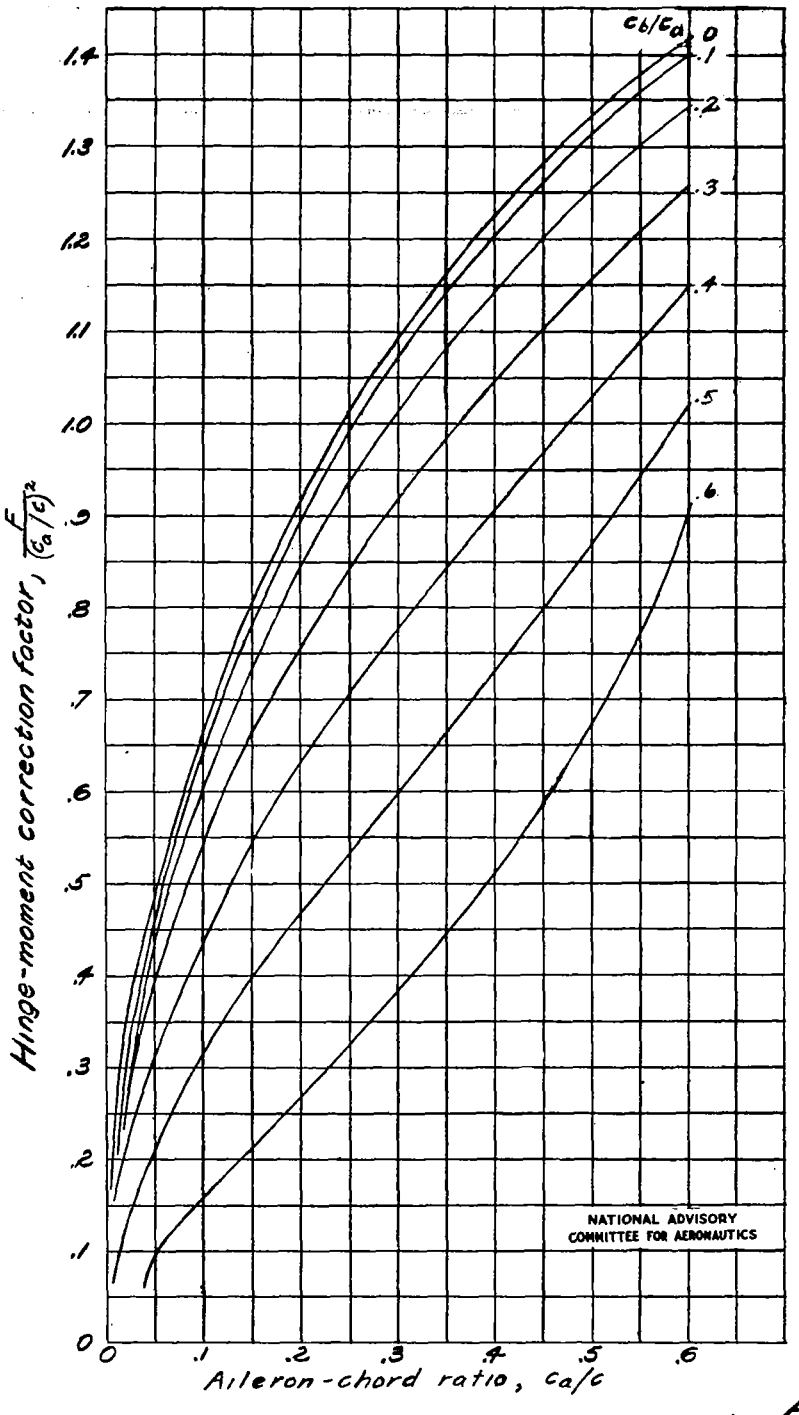

FIGURE 6.-Variation of the hinge-moment correction factor $\frac{F}{(c_a/c)^2}$ with aileron-chord ratio and external-overhang aerodynamic balance-chord ratio. For internal aerodynamic balance, use an effective $c_{b_e} = 0.8\, c_b$ (reference 5).

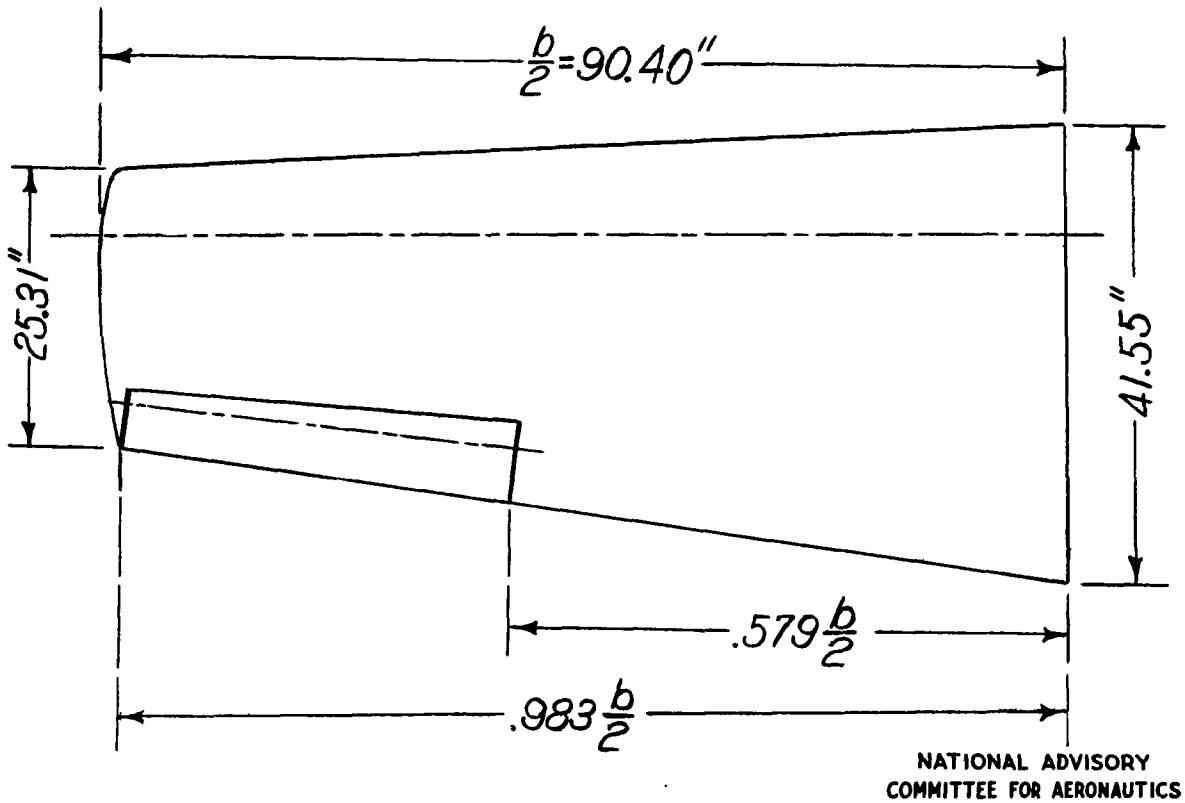

Figure 7.- Plan form of wing of model used for illustrative example.

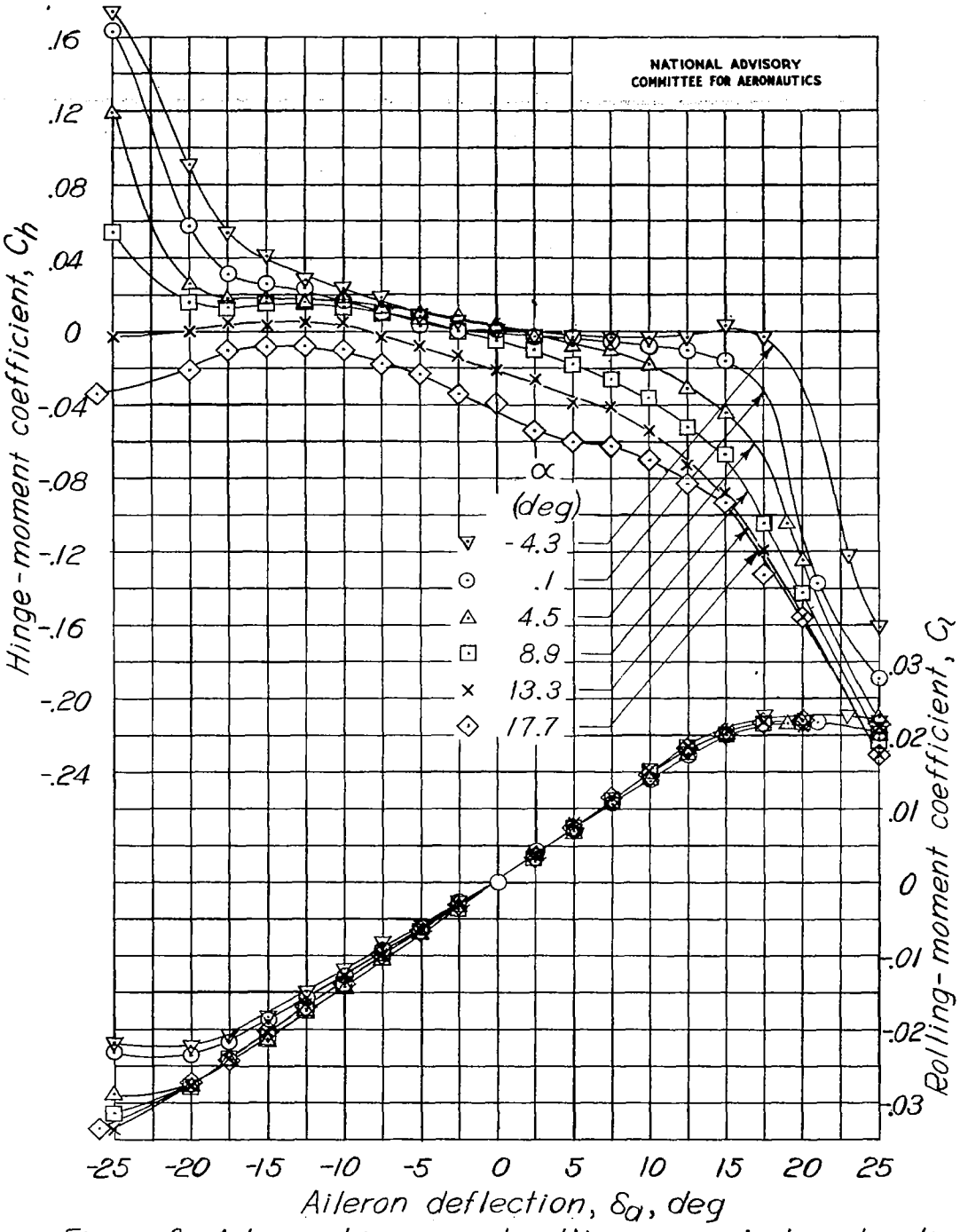

Figure 8.- Aileron hinge- and rolling-moment characteristics of the 0.40-scale model of the airplane used for the illustrative example. Characteristics plotted against aileron deflection.

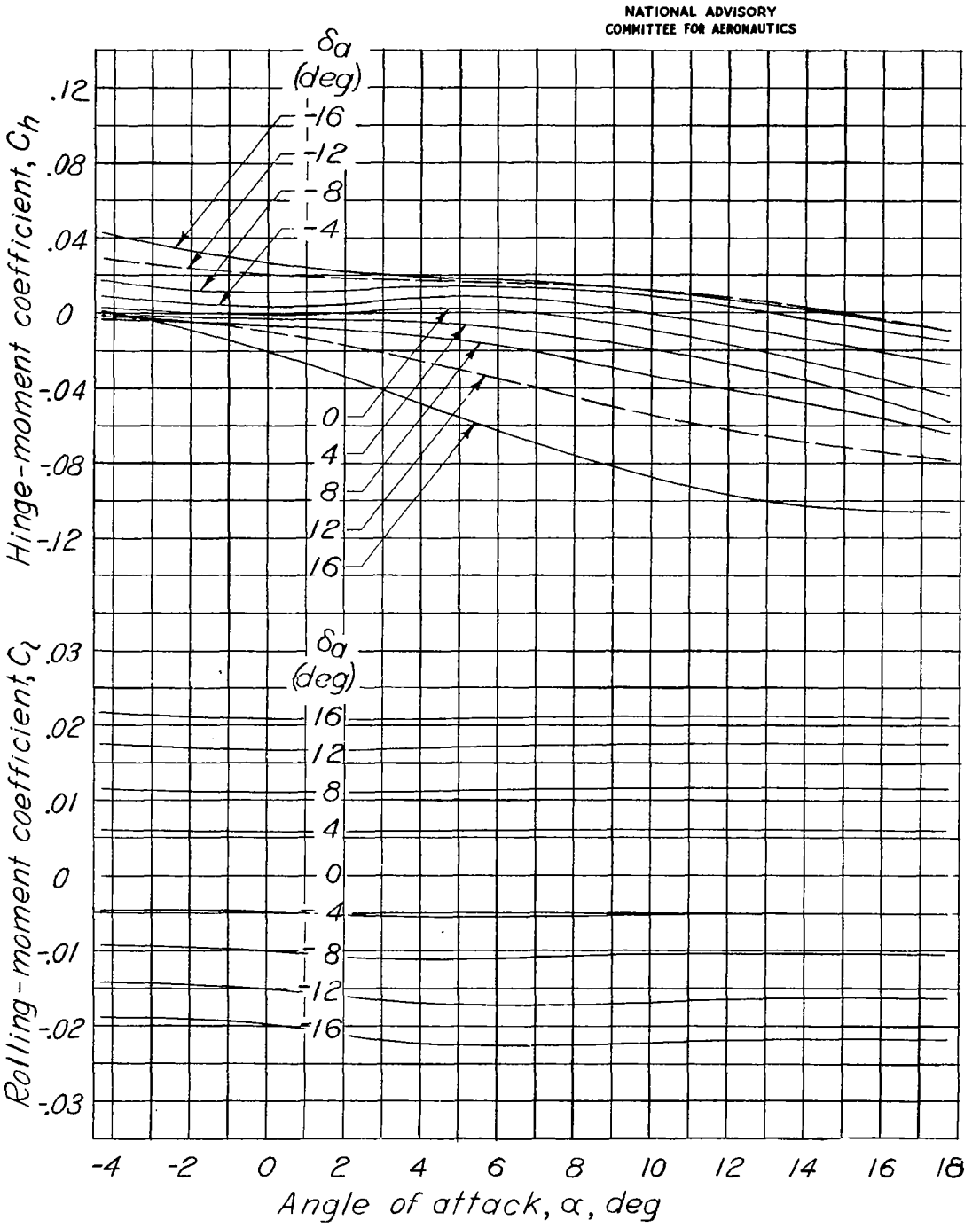

Figure 9.- Aileron hinge- and rolling-moment characteristics of the 0.40-scale model of the airplane used for the illustrative example. Characteristics plotted against angle of attack.

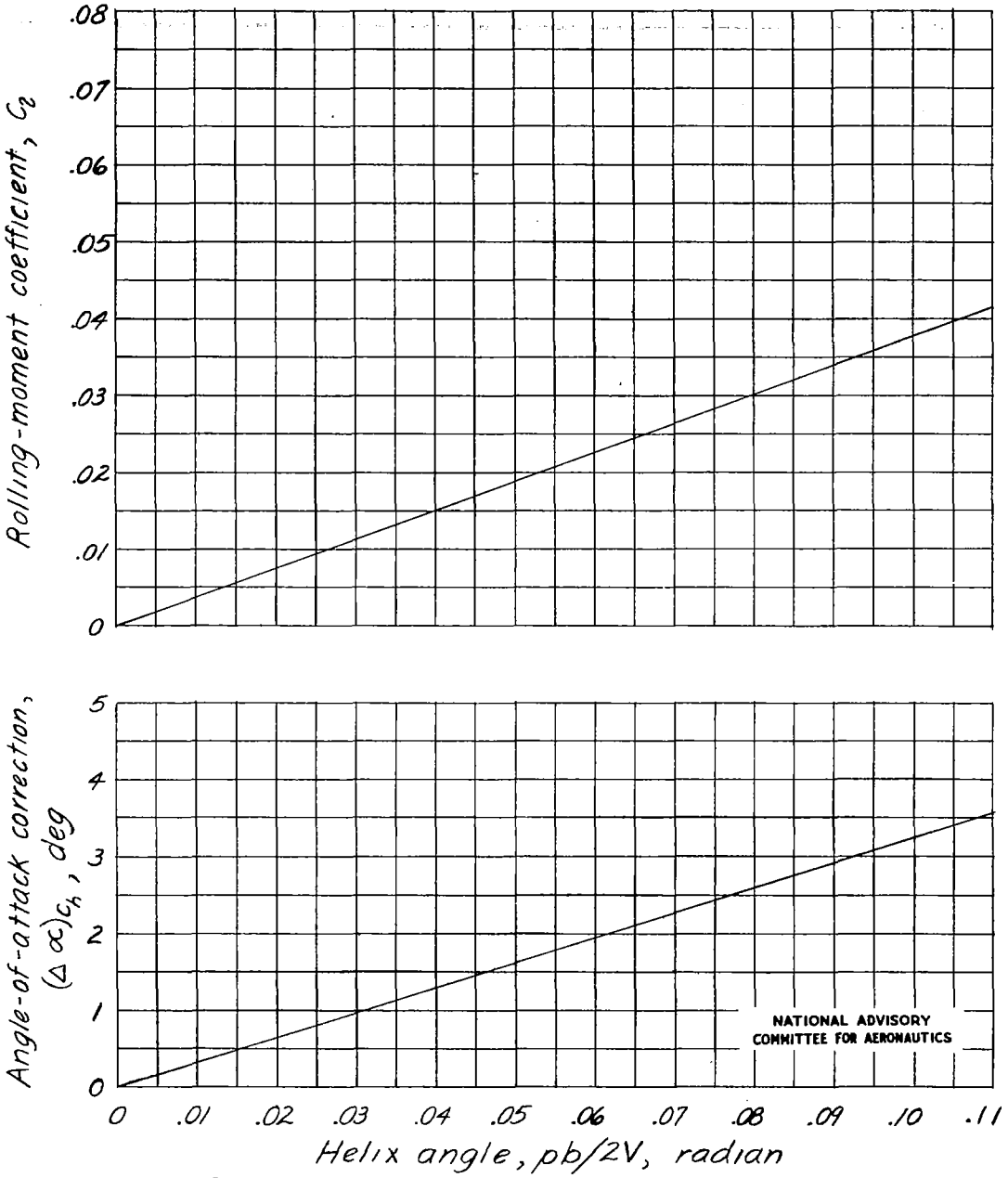

Figure 10.-Preliminary curves used in the computation of the wing-tip helix angles and the stick forces for the illustrative example.

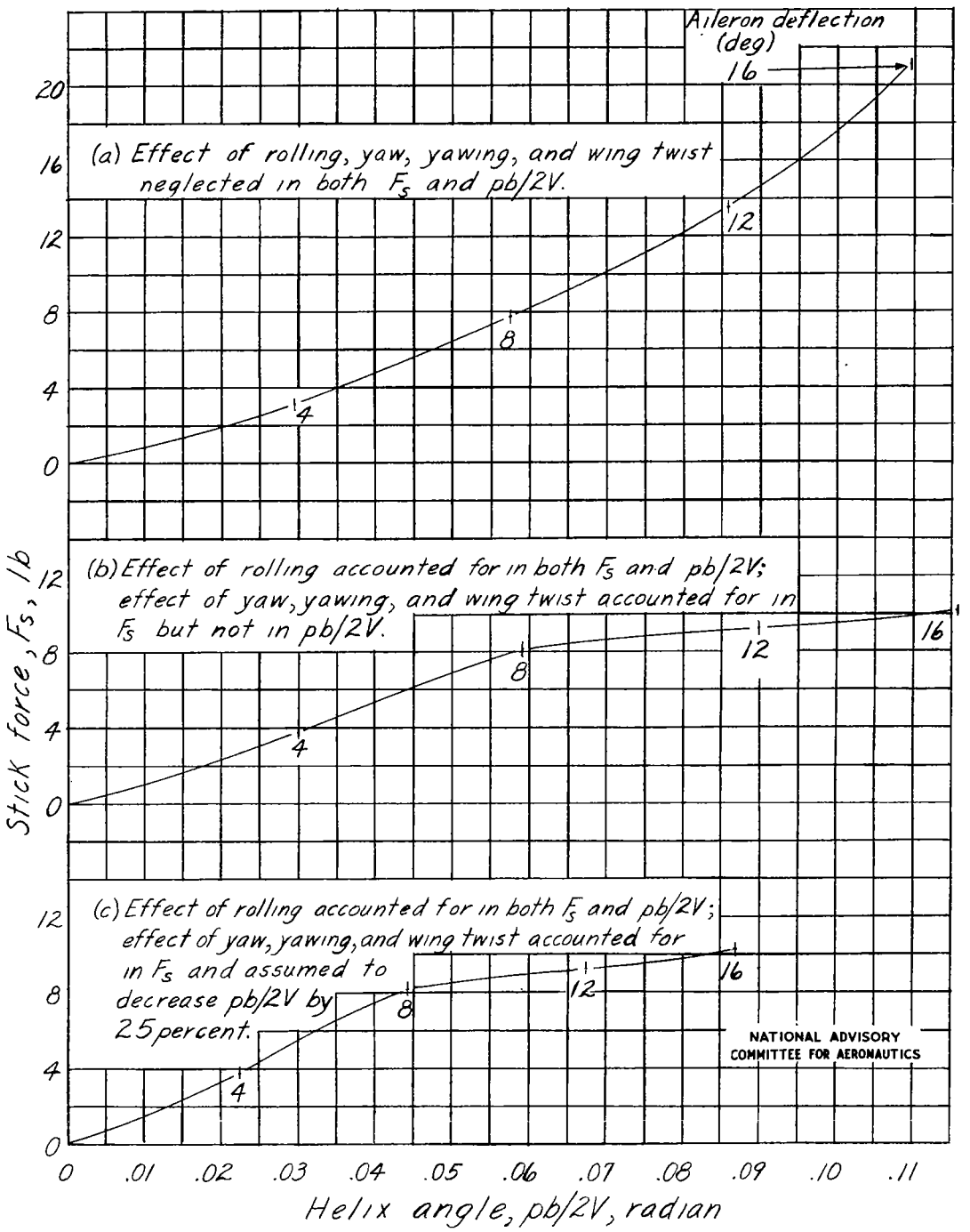

Figure 11.-Stick-force characteristics estimated for the airplane used for the illustrative example.

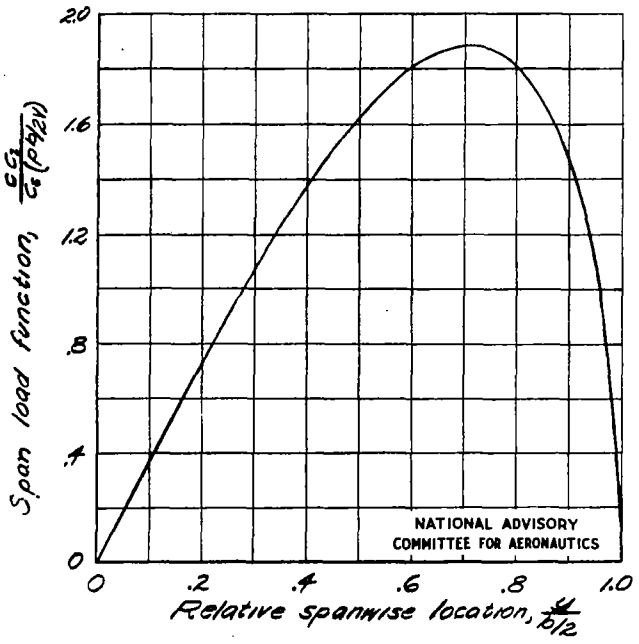

Figure 12.- Spanwise distribution of the span load or circulation function $\frac{cc_l}{c_s\left(\frac{pb}{2V}\right)}$ for a rolling elliptic wing of aspect ratio 6. (Determined from lifting-line theory.)

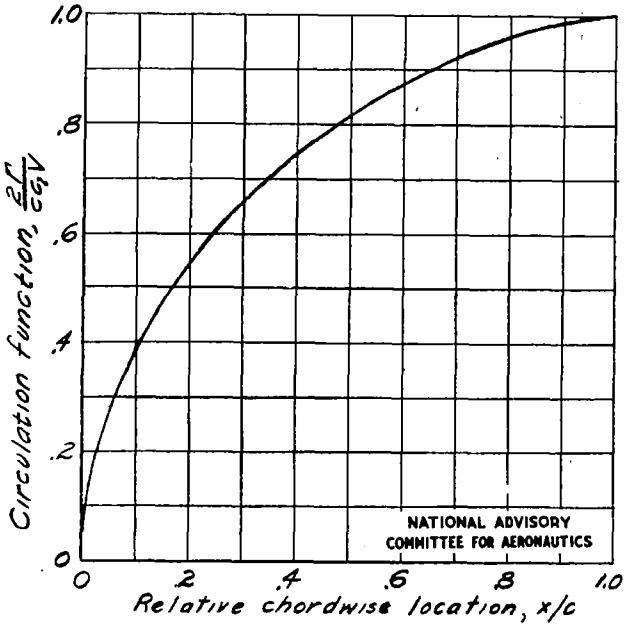

Figure 13.- Chordwise distribution of circulation function $\frac{2\Gamma}{cc_l V}$ for a flat plate. (Determined from thin-airfoil theory.)

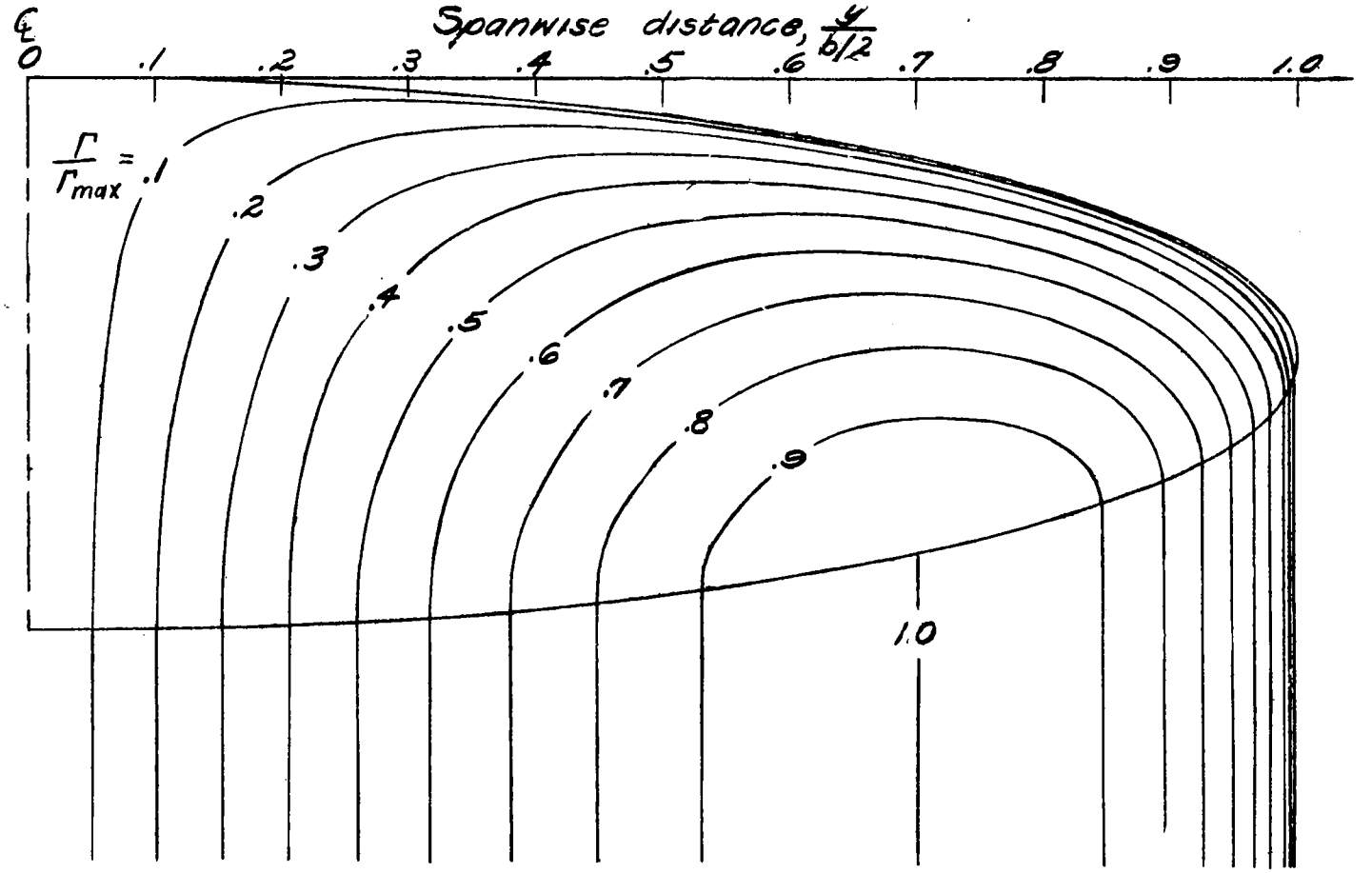

NATIONAL ADVISORY COMMITTEE FOR AERONAUTICS

$$\frac{\frac{2\Gamma}{c_s V\left(\frac{\rho b}{2V}\right)}}{\left[\frac{2\Gamma}{c_s V\left(\frac{\rho b}{2V}\right)}\right]_{max.}}$$

FIGURE 14.- Contour lines of the circulation function for an elliptic wing of aspect ratio 6 in steady roll.

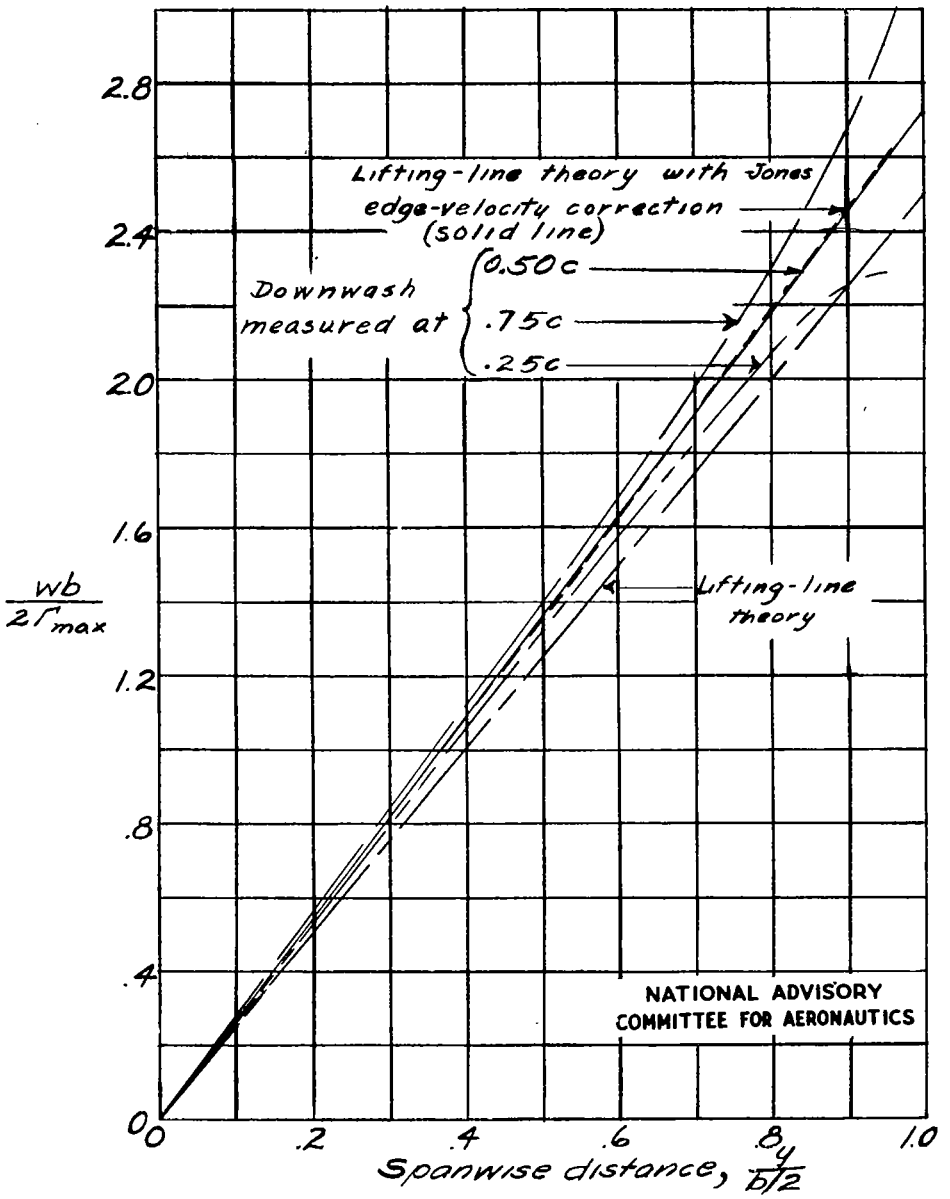

Figure 15.- Induced downwash function $wb/2\Gamma_{max}$ for an elliptical lifting surface of aspect ratio 6 in steady roll.

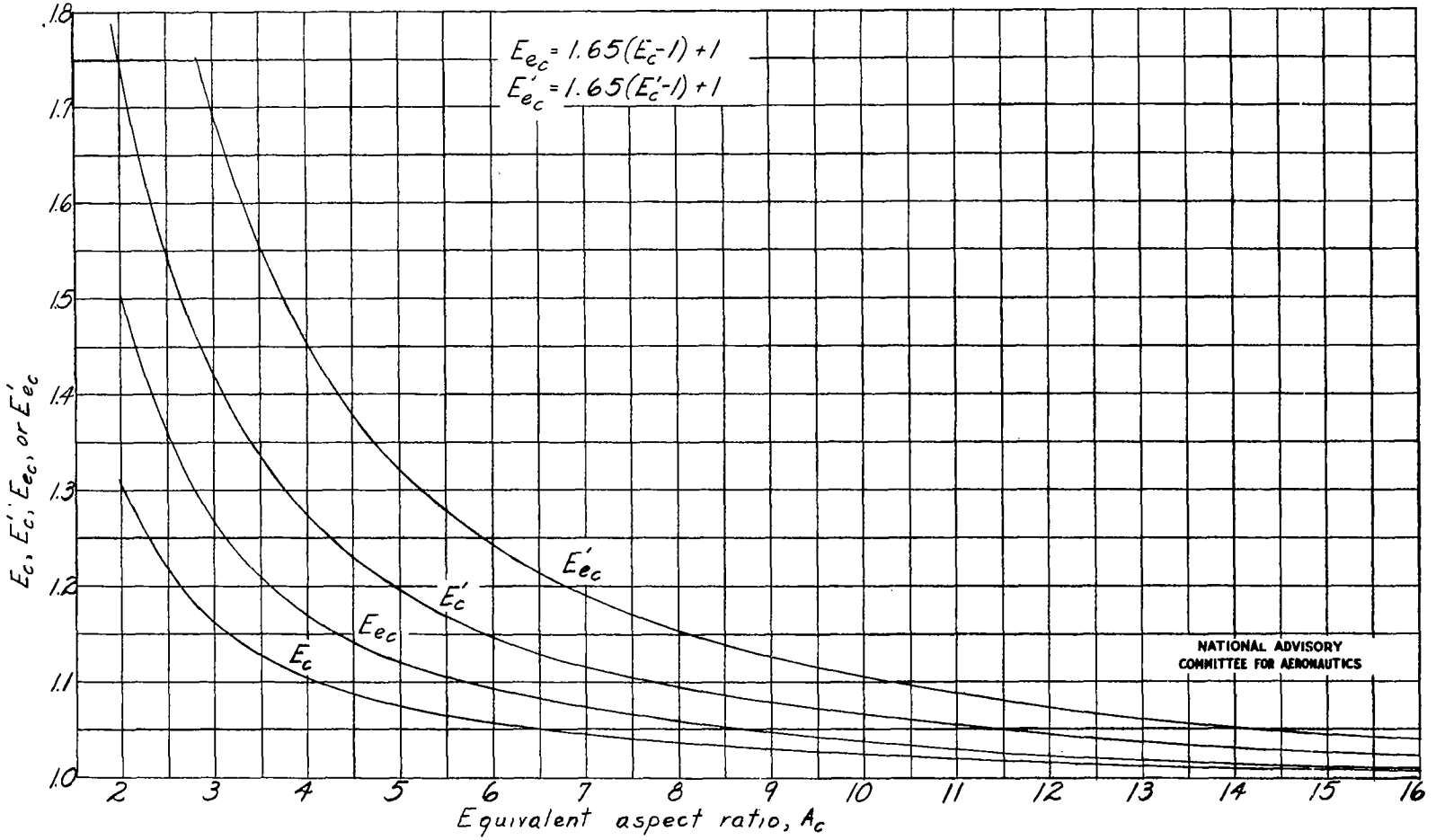

Figure 16.- Values of the Jones edge-velocity correction and the effective edge-velocity correction for elliptic wings at constant angle of attack and in steady roll. (Reference 1 and unpublished data.)

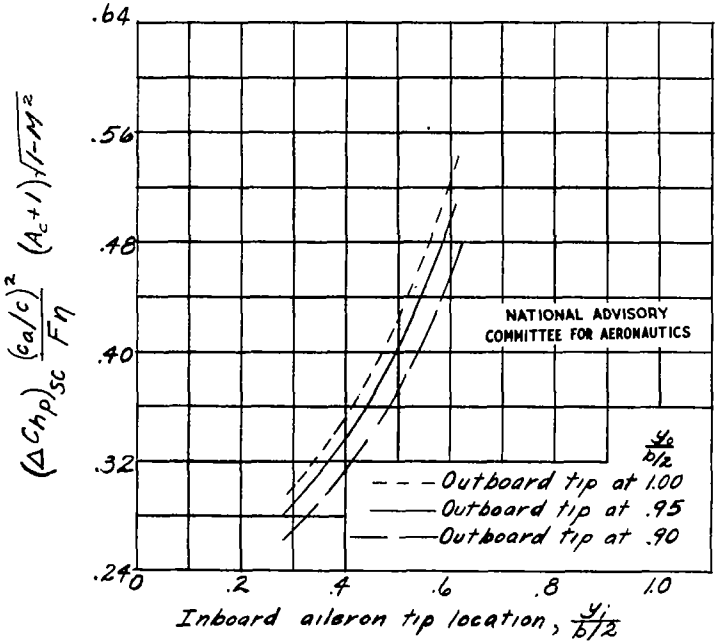

Figure 17.- Streamline-curvature correction to lifting-line-theory values C_{h_p} for thin elliptic wings estimated for any aspect ratio from electromagnetic-analogy data for wing of aspect ratio 6.

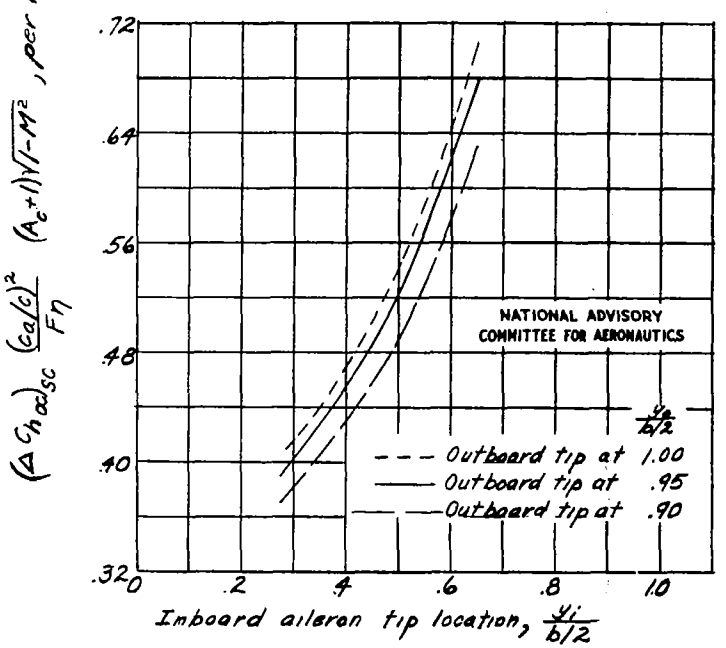

Figure 18.- Streamline-curvature correction to lifting-line-theory values of C_{h_α} for thin elliptic wings estimated for any aspect ratio from lifting-surface-theory calculations for wings of aspect ratios 3 and 6.

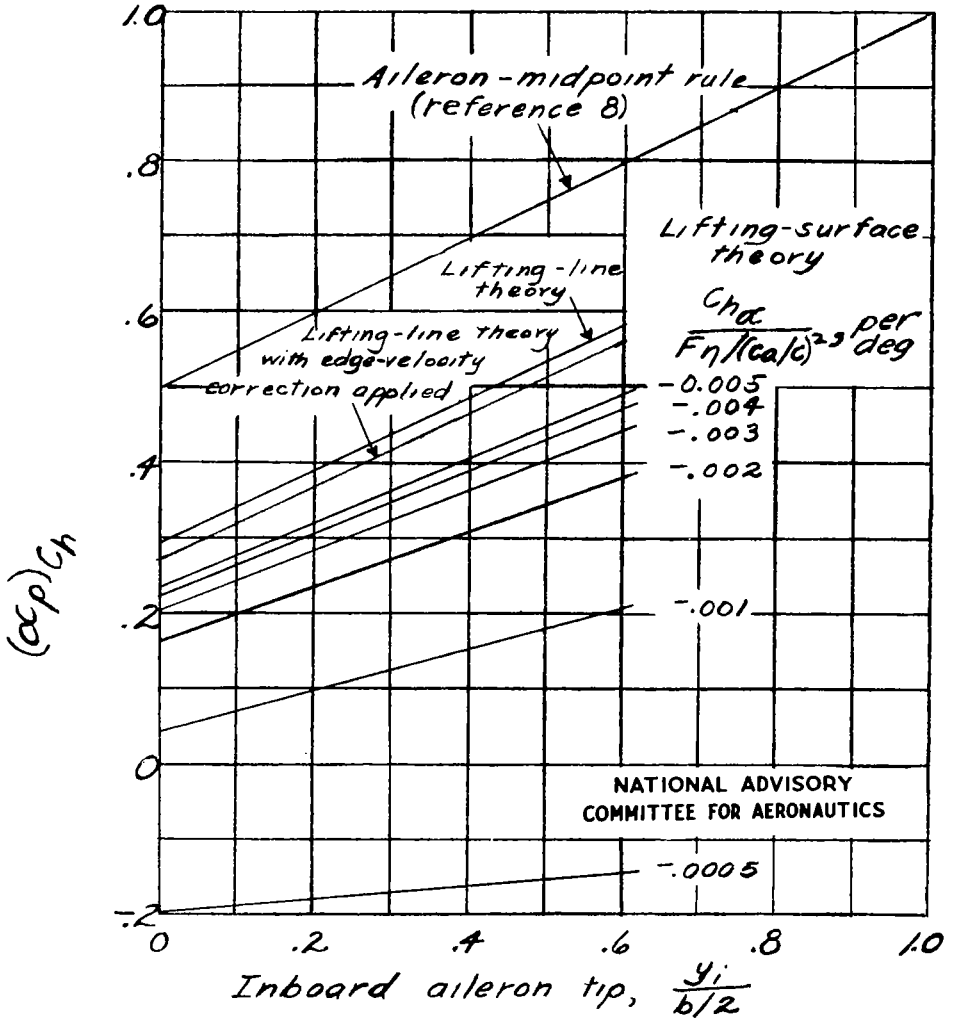

Figure 19.- Values of parameter $(\alpha_p)_{C_h}$ from aileron-midpoint rule, lifting-line theory, lifting-line theory with edge-velocity correction applied, and lifting-surface theory for an elliptic wing of aspect ratio 6. M = 0.